

Likelihood-based Changepoint Detection in Preferential Attachment Networks

BY DANIEL CIRKOVIC, TIANDONG WANG AND XIANYANG ZHANG

Department of Statistics, Texas A&M University, College Station, TX 77843, U.S.A

cirkovd@stat.tamu.edu, twang@stat.tamu.edu, zhangxiany@stat.tamu.edu

SUMMARY

Generative, temporal network models play an important role in analyzing the dependence structure and evolution patterns of complex networks. Due to the complicated nature of real network data, it is often naive to assume that the underlying data-generative mechanism itself is invariant with time. Such observation leads to the study of changepoints or sudden shifts in the distributional structure of the evolving network. In this paper, we propose a likelihood-based methodology to detect changepoints in undirected, affine preferential attachment networks, and establish a hypothesis testing framework to detect a single changepoint, together with a consistent estimator for the changepoint. The methodology is then extended to the multiple changepoint setting via both a sliding window method and a more computationally efficient score statistic. We also compare the proposed methodology with previously developed non-parametric estimators of the changepoint via simulation, and the methods developed herein are applied to modeling the popularity of a topic in a Twitter network over time.

Some key words: Changepoint detection; preferential attachment; likelihood ratio tests; social networks; martingale central limit theorem.

1. INTRODUCTION

In network analysis, understanding how a temporal network evolves is a consequential task. For example, assessing how interest in a topic diffuses over time in a Twitter network can only be evaluated if the network is observed temporally. Similarly, in order to judge how effective a policy is at dampening disease spread throughout a community, one must be able to compare the spread dynamics before and after the policy is instituted. Upon observing a large, temporal network, however, it is often naïve to assume that it evolved under one fixed data-generating process. Most temporal networks are exposed to forces, internal or external, that may augment the nature in which they evolve. Continuing the Twitter example, news of a major world event may receive increased interest, albeit for a short period of time, before returning to its pre-announcement popularity. These shifts in data-generating dynamics can be characterized as changepoints.

When it comes to modeling dynamic networks, one popular class of temporal, generative network models is the preferential attachment (PA) model. Since its initial emergence as the Barabási-Albert (BA) model in Barabási & Albert (1999), many generalizations have been developed in order to generate networks that better conform to real-world datasets; see for example Bollobás et al. (2003); Cirkovic et al. (2022); Gao et al. (2017); Wang & Resnick (2020). Estimating changepoints in the undirected preferential attachment model was first studied by Banerjee et al. (2018) and Bhamidi et al. (2018) where they employed non-parametric estimators of the changepoint based on fluctuations in the degree distribution. Although the methodology is

general, it does not directly determine the existence of changepoints. Real network datasets are inherently noisy objects and thus it is natural to ask whether a certain temporal shock has a large enough impact on the network formation, beyond what is typically expected, to be classified as a changepoint. Inspired by Banerjee et al. (2018) and Bhamidi et al. (2018), we propose likelihood-based alternatives to the changepoint problem, and provide a hypothesis testing framework that not only detects where a changepoint has occurred, but decides whether or not it even occurred in the first place. If a changepoint has not occurred, one may assume that the entire network is generated under a single PA process. Otherwise, different periods of time may have been governed by varying parameters under the preferential attachment evolution assumption.

In practice, it is possible to have multiple changepoints in a given data stream. Although it is justified theoretically, Banerjee et al. (2018) and Bhamidi et al. (2018) have not addressed the statistical nature of the multiple changepoint detection. Therefore, another goal of our work is to present efficient multiple changepoint detection algorithms that scale to massive networks. Outside of applications to the the PA model, the likelihood-based changepoint detection problem has a long history in the statistics literature. For an overview of both parametric and non-parametric changepoint detection methods, we refer to Csörgö et al. (1997). We also refer to Niu et al. (2016) for an overview of multiple changepoint procedures. In our present study, we provide two methods, namely sliding window and binary segmentation methods, to handle the multiple changepoint detection problem for PA networks, both of which have also been further applied to a real data example.

The rest of the paper is organized as follows. In Section 2, we provide important background information on the setup of the PA model and the likelihood-based inference. Then in Section 3.2, we establish the hypothesis testing framework for the single changepoint detection problem in the PA models, together with the proposal of a consistent estimator for the changepoint. We next discuss challenges and our resolutions (i.e. sliding window and binary segmentation methods) for the multiple changepoint situation in Section 4. A numerical study comparing the two proposed methods is also included in Section 4.3. Section 5 provides a real data example from a Twitter network, which gives an illustration of the applicability of our proposed methods. We give concluding remarks in Section 6, and all technical proofs are collected in the appendix.

2. PREFERENTIAL ATTACHMENT MODELING

2.1. *The standard preferential attachment model*

Preferential attachment (PA) has become a popular mechanism to model real-world, dynamic networks by imitating their scale-free behavior through a “rich-get-richer” data-generative mechanism. In this section, we review well-known aspects of the undirected preferential attachment model (see Chapter 8 of Van Der Hofstad (2017) for a full treatment).

For our theoretical analyses, we assume the graph sequence $\{G(k)\}_{k=2}^n$ is initialized with two nodes connected by two edges, i.e. $G(2) \equiv (V(2), E(2))$ where $V(2) = \{1, 2\}$ and $E(2) = \{\{1, 2\}, \{1, 2\}\}$. From $G(k-1)$ to $G(k)$, $k \geq 3$, a new node k together with an undirected edge, $\{k, v_k\}$, is added to the graph according to the following preferential attachment rule. For $v_k \in V(k-1)$ and $k \geq 3$,

$$\mathbb{P}(\{k, v_k\} \in E(k) \setminus E(k-1) \mid \mathcal{F}_{k-1}) = \frac{D_{v_k}(k-1) + \delta}{(2 + \delta)(k-1)}, \quad (1)$$

where $D_{v_k}(k-1)$ denotes the degree of node $v_k \in V(k-1)$ and \mathcal{F}_k is the sigma algebra generated by the information in $G(k)$. Note that we exclude the possibility of having self-loops in

the model setup. In order for (1) to result in a valid pmf, it is further assumed that $\delta > -1$. In what follows, we employ the short-hand notation $\text{PA}(\delta)$ to denote this process.

For $i \geq 1$, let $N_i(k) = \sum_{w \in V(k)} 1_{\{D_w(k)=i\}}$ be the number of nodes with degree i at time k . By (Van Der Hofstad, 2017, Theorem 3.8), we have

$$\frac{N_i(k)}{k} \xrightarrow{a.s.} p_i(\delta) = (2 + \delta) \frac{\Gamma(3 + 2\delta)\Gamma(i + \delta)}{\Gamma(1 + \delta)\Gamma(i + 3 + 2\delta)} \quad \text{as } k \rightarrow \infty. \quad (2)$$

Also, let $N_{>i}(k) := \sum_{j>i} N_j(k)$ be the number of nodes with degree greater than i at time k , then we have that

$$\frac{N_{>i}(k)}{k} \xrightarrow{a.s.} p_{>i}(\delta) = \frac{\Gamma(3 + 2\delta)\Gamma(i + 1 + \delta)}{\Gamma(1 + \delta)\Gamma(i + 3 + 2\delta)} \quad \text{as } k \rightarrow \infty. \quad (3)$$

From (2) and (3), we have the following convenient identity:

$$p_{>i}(\delta) = \frac{(i + \delta)p_i(\delta)}{2 + \delta}, \quad (4)$$

which is helpful later in the proof of our main results. By Stirling's formula, $p_i(\delta) \sim C i^{-(3+\delta)}$ as $i \rightarrow \infty$, where $C = (2 + \delta)\Gamma(3 + 2\delta)/\Gamma(1 + \delta)$, giving the PA model the ability to exhibit scale free behavior (see Chapter 8.4 of Van Der Hofstad, 2017, for more details).

2.2. Likelihood inference

In this section, we will review likelihood-based inference for the preferential attachment model. Likelihood inference for the undirected affine preferential attachment model was rigorously studied in Gao & van der Vaart (2017) and will form the basis for our changepoint analyses. Assume we have observed the graph sequence $\{G(k)\}_{k=2}^n$ evolving according to the classical rule in (1) with $\delta \in [\eta, K]$, where $\eta > 1$ and $K < \infty$. The likelihood of δ given the entire graph sequence is given by

$$L(\delta \mid \{G(k)\}_{k=2}^n) = \prod_{k=3}^n \frac{D_{v_k}(k-1) + \delta}{(2 + \delta)(k-1)}. \quad (5)$$

Since we will later consider model evolution with changepoints, it is convenient to denote the likelihood function:

$$L_{(ns, nt]}(\delta) := L\left(\delta \mid \{G(k)\}_{k=\lfloor ns \rfloor + 1}^{\lfloor nt \rfloor}\right), \quad \text{for } s, t \in [0, 1], s < t.$$

If s is such that the likelihood product in (5) is indexed for $k < 3$, we simply denote the multiples as 1. The log-likelihood becomes

$$\begin{aligned} \ell_{(ns, nt]}(\delta) &:= \log L_{(ns, nt]}(\delta) \\ &= \sum_{k=\lfloor ns \rfloor + 1}^{\lfloor nt \rfloor} \log(D_{v_k}(k-1) + \delta) - \sum_{k=\lfloor ns \rfloor + 1}^{\lfloor nt \rfloor} \log(k-1) - (\lfloor nt \rfloor - \lfloor ns \rfloor) \log(2 + \delta), \end{aligned} \quad (6)$$

which emits score and hessian

$$u_{(ns, nt]}(\delta) := \frac{\partial}{\partial \delta} \ell_{(ns, nt]}(\delta) = \sum_{k=\lfloor ns \rfloor + 1}^{\lfloor nt \rfloor} \frac{1}{D_{v_k}(k-1) + \delta} - \frac{\lfloor nt \rfloor - \lfloor ns \rfloor}{2 + \delta}, \quad (7)$$

$$u'_{(ns, nt]}(\delta) := \frac{\partial^2}{\partial \delta^2} \ell_{(ns, nt]}(\delta) = - \sum_{k=\lfloor ns \rfloor + 1}^{\lfloor nt \rfloor} \frac{1}{(D_{v_k}(k-1) + \delta)^2} + \frac{\lfloor nt \rfloor - \lfloor ns \rfloor}{(2 + \delta)^2}. \quad (8)$$

We thus define the maximum likelihood estimator based on the edges $\lfloor ns \rfloor + 1$ to $\lfloor nt \rfloor$, $\hat{\delta}_{(ns, nt]}$, as the solution to the equation $u_{(ns, nt]}(\delta) = 0$. If we are using the full data to estimate δ , we will employ the notation $\hat{\delta}_n := \hat{\delta}_{(0, n]}$. It is proven in Gao & van der Vaart (2017) that for fixed s and t $\hat{\delta}_{(ns, nt]}$ is a consistent estimator of δ . The asymptotic normality of $\hat{\delta}_{(ns, nt]}$ under $\text{PA}(\delta)$ is derived in Lemma 1, which is crucial in the derivation of our likelihood ratio test.

3. CHANGEPOINT DETECTION

Although the classical preferential attachment model is already a popular choice for modeling real-world networks, it essentially assumes the network evolution rule (cf. (1)) to remain unchanged over time and is not perturbed by temporal shocks to the network. For many real-life scenarios, this is an unrealistic assumption (see for instance the Twitter data example in Section 5). In order to capture these dynamics, a preferential attachment model with changepoints have been proposed in Bhamidi et al. (2018), which we now summarize. The graph sequence $\{G(k)\}_{k=2}^n$ evolves as follows:

- For $k = 2, \dots, \lfloor nt^* \rfloor$, allow the network evolve according to $\text{PA}(\delta_1)$.
- For $k = \lfloor nt^* \rfloor + 1, \dots, n$, the network evolves according to $\text{PA}(\delta_2)$ where $G(\lfloor nt^* \rfloor)$ is used as the seed graph.

In the rest of this paper, we refer to this graph evolution process as $\text{PA}(t^*; \delta_1, \delta_2)$ with $\delta_1 \neq \delta_2$. The shift from δ_1 to δ_2 thus signifies that some disturbance has occurred at time $\lfloor nt^* \rfloor + 1$, and has affected the underlying structure of the network evolution going forward.

3.1. Non-parametric methods

In order to detect the changepoint t^* under the $\text{PA}(t^*; \delta_1, \delta_2)$ model, Bhamidi et al. (2018) employs a non-parametric estimator which tracks the proportion of nodes with degree 1 (i.e. leaves) as the network evolves. In a later paper, (Banerjee et al., 2018) develops a non-parametric estimator for t^* under more general conditions on the attachment rule (1). As opposed to Bhamidi et al. (2018), the methodology in Banerjee et al. (2018) tracks changes in the entire empirical degree distribution, which in-turn provides more information about the changepoint location. Hence, for brevity, we only present and compare our likelihood-based methods to Banerjee et al. (2018). Although their theory is based on a preferential attachment model where nodes attach according to their out-degree rather than their total degree, their methodology is still valid for the linear PA case since the associated δ parameters would just differ by 1.

The estimator of the changepoint t^* in Banerjee et al. (2018) is given by

$$\hat{T}_n = \inf \left\{ t \geq \frac{1}{h_n} : \sum_{i=0}^{\infty} 2^{-i} \left| \frac{N_{i+1}(\lfloor nt \rfloor)}{nt} - \frac{N_{i+1}(\lfloor n/h_n \rfloor)}{n/h_n} \right| > \frac{1}{b_n} \right\}, \quad (9)$$

where h_n and b_n are intermediate sequences such that $h_n \rightarrow \infty$, $b_n \rightarrow \infty$, $\frac{h_n}{n} \rightarrow 0$ and $\frac{b_n}{n} \rightarrow 0$ as $n \rightarrow \infty$. Intuitively, (9) detects a changepoint when the \mathbb{R}_+^∞ distance between the empirical degree distributions after the changepoint and some time in the distant past exceeds a given threshold. As reasonable defaults, Banerjee et al. (2018) recommends using $h_n = \log \log n$ and $b_n = n^{1/\log \log n}$ which we will also follow. The consistency of \hat{T}_n has been justified in Banerjee et al. (2018) as well, i.e. $\hat{T}_n \xrightarrow{P} t^*$, provided that there is a changepoint at t^* . Although methods developed in (Banerjee et al., 2018) are applicable to a wide range of sublinear preferential attachment models, in their current state they do not provide a mechanism to test if a changepoint has occurred in the first place, motivating the need for a hypothesis testing framework and other likelihood-based alternatives.

3.2. Likelihood ratio test

As mentioned earlier, the goal of statistical changepoint detection is two-fold. We need to first decide if a changepoint has occurred, and if so, where it occurred. Both of these objectives can be conveniently met in a hypothesis testing framework. Consider the hypotheses

$$\begin{aligned} H_0 : & \text{The graph sequence } \{G(k)\}_{k=2}^n \text{ evolves according to PA}(\delta). \\ H_A : & \exists t^* \in [\gamma, 1 - \gamma] \text{ such that } \{G(k)\}_{k=2}^n \text{ evolves according to PA}(t^*, \delta_1, \delta_2) \end{aligned} \quad (10)$$

for some $\gamma \in (0, 1/2)$. Clearly, the alternative hypothesis implies the existence of a changepoint, while the null hypothesis assumes that the network is generated according to the PA rule (1) via a fixed δ . Under H_A , γ ensures that the changepoint is bounded away from 0 and 1. In practice, this assumption guarantees that a sufficient number of edges is generated under both PA schemes (allowing for accurate estimation of δ_1 and δ_2), but also plays a theoretical role in later proofs.

To test (10), we consider the likelihood ratio

$$\Lambda_m := \frac{L_{(0,n]}(\hat{\delta}_n)}{L_{(0,m]}(\hat{\delta}_{(0,m]})L_{(m,n]}(\hat{\delta}_{(m,n]})} \quad \text{for } m = \lfloor n\gamma \rfloor, \dots, \lfloor n(1 - \gamma) \rfloor. \quad (11)$$

The numerator in (11) maximizes the likelihood under the null hypothesis of no changepoint and the denominator is maximized under the alternative $\delta_1 \neq \delta_2$ for some conjectured changepoint location m . For theoretical analyses, it is instead convenient to work with the statistic $-2 \log \Lambda_m$. With this transformation, a large value of $-2 \log \Lambda_m$ provides evidence in favor of a changepoint located at m . Therefore, one may expect the m that maximizes $-2 \log \Lambda_m$ under the alternative to satisfy $m/n \approx t^*$ as $n \rightarrow \infty$.

In order to derive the asymptotic distribution for the maximum of $-2 \log \Lambda_m$ under the null hypothesis, it is amenable to convert to continuous time and consider a stochastic process perspective. Consider the log-likelihood ratios $-2 \log \Lambda_{\lfloor nt \rfloor}$ indexed by $t \in [\gamma, 1 - \gamma]$. This is a right-continuous process, and hence an element of the Skorohod space $D[\gamma, 1 - \gamma]$ which we will equip with the Skorohod metric. When the limiting process of $-2 \log \Lambda_{\lfloor nt \rfloor}$ is derived, the continuous mapping theorem gives the asymptotic distribution of the supremum of $-2 \log \Lambda_{\lfloor nt \rfloor}$ for $t \in [\gamma, 1 - \gamma]$.

The following theorem gives the asymptotic distribution of

$$\sup_{t \in [\gamma, 1 - \gamma]} -2 \log \Lambda_{\lfloor nt \rfloor},$$

under H_0 , from which we derive the hypothesis test.

THEOREM 1. Fix $\gamma \in (0, 1/2)$. Then under H_0 in (10)

$$\sup_{t \in [\gamma, 1-\gamma]} -2 \log \Lambda_{nt} \Rightarrow \sup_{t \in [\gamma, 1-\gamma]} \frac{B^2(t)}{t(1-t)}, \quad (12)$$

in \mathbb{R} , where \Rightarrow denotes the weak convergence.

We defer the detailed proof of Theorem 1 to Appendix A.1. In fact, Theorem 1 establishes a hypothesis testing framework for the null of no changepoint, rejects H_0 when the test statistics

$$\sup_{t \in [\gamma, 1-\gamma]} -2 \log \Lambda_{nt}$$

exceeds the $(1 - \alpha)$ -th quantile of the limiting distribution,

$$\sup_{t \in [\gamma, 1-\gamma]} \frac{B^2(t)}{t(1-t)}.$$

Though quantiles of the limit distribution are not readily available in most software, they can be simulated via Brownian motion realizations or approximations like that of Equation (1.3.26) in Csörgö et al. (1997).

Now that Theorem 1 gives us the ability to detect the presence of a changepoint, we would like to consistently estimate it. As mentioned earlier, large values of $-2 \log \Lambda_{[nt]}$ indicate that t is likely a changepoint. Hence, under H_A , we expect the argmax of $-2 \log \Lambda_{[nt]}$ to be a consistent estimator of the true changepoint t^* , and Theorem 2 formalizes these notions.

THEOREM 2. Fix $\gamma \in (0, 1/2)$ and assume that there exists only one changepoint at $t^* \in [\gamma, 1 - \gamma]$. Suppose also that the network evolves according to $PA(t^*; \delta_1, \delta_2)$. Then we have

$$\hat{t}_n := n^{-1} \arg \max_{[n\gamma] \leq m \leq [(1-\gamma)n]} -2 \log \Lambda_m \xrightarrow{p} t^*, \quad (13)$$

as $n \rightarrow \infty$.

We leave the proof of Theorem 2 to Appendix A.4, and provide comparisons on the performance of \hat{t}_n and \hat{T}_n through a simulation study in the next section.

3.3. Simulation study

Though the consistency of \hat{t}_n and \hat{T}_n has been justified, we now further evaluate and compare their numerical performance on simulated data. In each simulation, the preferential attachment networks are initialized by a node with a self-loop, and all simulations assume a typical significance level of $\alpha = 0.05$. We first assess the Type 1 error rate for the likelihood ratio methodology by simulating 500 $PA(\delta)$ networks with 50,000 edges, $\delta \in \{-0.5, 0, 1, 2\}$ and $\gamma = 0.1$. The Type 1 error rates and their Bernoulli-based standard errors are presented in Table 1. As expected, the Wald-based confidence intervals for the rejection rates all contain $\alpha = 0.05$. Hence, the asymptotic distribution in Theorem 1 is a good approximation for the distribution of the likelihood ratio under the null hypothesis, even at small sample sizes. Most real-world dynamic networks (e.g. those listed on data repositories like SNAP Leskovec & Krevl (2014) and KONECT Kunegis (2013)) contain well over 50,000 edges and hence asymptotic approximations are reliable, assuming the network is truly generated by a PA process.

Next, we evaluate the statistical power and estimation of the changepoint location for the likelihood ratio methodology. We apply the likelihood ratio test to 500 simulated $PA(0.6; 0, \delta_2)$ networks, i.e. they are initialized by a Barabási-Albert process, $PA(0)$, and then transitions to a $PA(\delta_2)$ process at $t^* = 0.6$. The networks have 50,000 edges and we again let $\gamma = 0.1$. Here,

δ	-0.5	0	1	2
Rejection Rate	0.050	0.042	0.046	0.052
Standard Error	0.0097	0.0090	0.0094	0.0099

Table 1. *Rejection rates and (Bernoulli-based) standard errors for the likelihood ratio test applied to 500 PA(δ) networks with 50,000 edges and $\gamma = 0.1$.*

we allow δ_2 to vary between -0.2 and 0.2 by increments of 0.02 . An empirical power curve and mean absolute error for the changepoint location for tests that rejected the null hypothesis are presented in Figure 1. The likelihood ratio methodology is powerful; differences in the offset parameter beyond 0.1 in absolute value are detected well-over 95% of the time. Interestingly, decreases in the offset parameter are detected slightly more often than increases. For differences in the offset parameter below 0.1 in absolute value, however, the estimation of the changepoint location becomes unreliable.

In order to further assess the accuracy of the changepoint location estimate, we compare the estimation error for the likelihood ratio and non-parametric estimators, \hat{t}_n and \hat{T}_n , on larger networks with greater, more realistic differences in the offset parameter. Specifically, we simulate 500 networks of size 100,000 from a PA($0.6; 0, \delta_2$) process, where δ_2 is allowed to range from 0.1 to 0.5 by increments of 0.1 . The mean absolute error in changepoint location is presented in Table 2. The likelihood ratio test rejects the null hypothesis in all simulations. Compared to previous simulations, \hat{t}_n becomes highly accurate with larger differences in the offset parameter and has uniformly smaller error than \hat{T}_n . The small differences in the offset parameter require the addition of many nodes to manifest in the empirical degree distribution according to the law of large numbers effect, hence \hat{T}_n performs poorly for small δ_2 . We also remark here that the supremacy of the likelihood ratio is unsurprising, since the likelihood-based methodology should out-perform non-parametric procedures when the data-generating model is correctly specified.

The non-parametric estimator \hat{T}_n , however, was designed to accommodate more general preferential attachment models. Namely, \hat{T}_n can detect differences between sublinear regimes of preferential attachment as explained in Assumption 2.1 of Banerjee et al. (2018). In order to assess the robustness of the likelihood ratio methodology to more general changes in the degree-based attractiveness of nodes, we generate 500 networks with 100,000 edges, where the attachment function changes from linear to sublinear at $t^* = 0.6$. At step k , node v is chosen to be attached to with probability proportional to $D_v(k-1) + 1$ for $k \leq \lfloor nt^* \rfloor$, and $(D_v(k-1) + 1)^b$ for $k \geq \lfloor nt^* \rfloor + 1$. Here we allow $b \in \{0.5, 0.6, 0.7, 0.8, 0.9\}$, where larger values of b thus indicate less dramatic changes in the attachment function. Mean absolute errors (MAE) in changepoint location for \hat{t}_n and \hat{T}_n are reported in Table 3. Although $\hat{\delta}_{(nt,n]}$ is generally computed under a misspecified model, the likelihood ratio methodology still performs well by virtue of $\hat{\delta}_{(0,nt]}$ and $\hat{\delta}_{(nt,n]}$ being far apart near the true changepoint. The non-parametric estimator \hat{T}_n performs well for lower values of b , but if the change in attachment function is subtle, it performs worse. This simulation, along with the previous, indicates that the empirical degree distribution is not sensitive to small changes in the attachment function from a statistical perspective.

4. MULTIPLE CHANGEPOINT DETECTION

So far our study only focuses on the case with a single changepoint, but for pragmatic purposes, it is important to consider the generalization to circumstances with multiple changepoints. We start with discussions on some difficulties that the methodology presented in Section 3.2 may

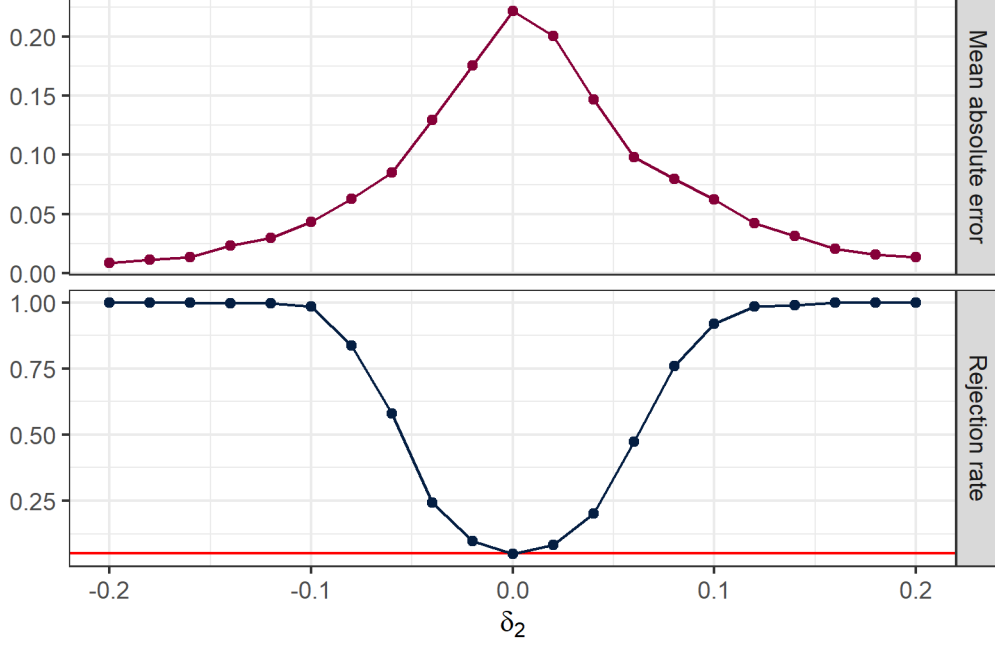


Fig. 1. Empirical rejection rates for the likelihood ratio test applied to 500 $PA(0.6; 0, \delta_2)$ networks with 50,000 edges and $\gamma = 0.1$ along with average absolute error for change-point location. Error is only computed for those tests that reject the null hypothesis. Red line indicates $\alpha = 0.05$.

δ_2	0.1	0.2	0.3	0.4	0.5
$MAE(\hat{t}_n)$	0.0281	0.0070	0.0030	0.0018	0.0013
$MAE(\hat{T}_n)$	0.2574	0.1518	0.0930	0.0710	0.0560

Table 2. Empirical mean absolute error of \hat{t}_n and \hat{T}_n for 500 $PA(0.6; 0, \delta_2)$ networks with 100,000 edges and $\gamma = 0.1$.

b	0.5	0.6	0.7	0.8	0.9
$MAE(\hat{t}_n)$	0.0004	0.0005	0.0009	0.0019	0.0079
$MAE(\hat{T}_n)$	0.0343	0.0440	0.0607	0.0969	0.2320

Table 3. Empirical mean absolute error for \hat{t}_n and \hat{T}_n for 500 networks initialized by a $PA(1)$ process which transitions to a sublinear PA process with attachment function $(\text{Degree} + 1)^b$ at $t^* = 0.6$. Networks are of 100,000 edges, and we choose $\gamma = 0.1$.

face when applied to the multiple changepoint setting and present an alternative strategy to detect multiple changepoints. The consideration of multiple changepoints can not only accentuate difficulties faced in the single changepoint case, but also introduce new complications. Akin to the single changepoint case, statistical multiple changepoint detection is often presented under the hypothesis testing framework, a convention that we will follow Chakraborty & Zhang (2021); Niu et al. (2016).

Fix $\gamma \in (0, 1/2)$ and consider the hypothesis test

$$\begin{aligned} H_0 : & \text{The graph sequence } \{G(k)\}_{k=2}^n \text{ evolves according to PA}(\delta). \\ H_A : & \text{There exists a partition } \gamma < t_1^* < \dots < t_\tau^* < 1 - \gamma \text{ such that } \{G(k)\}_{k=2}^n \\ & \text{evolves according to PA}(t_1^*, \dots, t_\tau^*; \delta_1, \dots, \delta_{\tau+1}) \end{aligned} \quad (14)$$

Here $\text{PA}(t_1^*, \dots, t_\tau^*; \delta_1, \dots, \delta_{\tau+1})$ is the natural extension of the model presented in Section 3 but now jumps occur at edges $\lfloor nt_1^* \rfloor, \dots, \lfloor nt_\tau^* \rfloor$ with the initializer process being $\text{PA}(\delta_1)$. Note that H_0 in (14) matches that of (10), implying that if the null hypothesis is true, the same exact methodology from Section 3.2 can be applied. Jointly estimating the changepoints under H_A is a difficult task, and hence the task of finding multiple changepoints is often reduced to sequentially uncovering changepoints one at a time. That is, the multiple changepoint detection problem is reduced to a sequence of single changepoint detection problems.

4.1. Screening and Ranking (SaRa)

One popular way decomposing the multiple changepoint problem to a sequence of single changepoint problems is via local estimation of the multiple changepoints. When applying likelihood ratio methodology, it is pertinent to ensure that the model is correctly specified. Naively applying the sequence of statistics (11) to a graph sequence with multiple changepoints will result in portions of the edgelist that are specified as a single PA process, though they are truly governed by multiple PA processes. Under the alternative, this leads to suboptimal estimation of model parameters, and thus suboptimal statistics and hypothesis tests. Instead, to ensure test regions contain at most one changepoint, Hao et al. (2013) and Niu & Zhang (2012) proposed a screening-and-ranking (SaRa) algorithm to detect multiple changepoints. In effect, the SaRa algorithm decomposes the hypothesis test (14) into a sequence of hypotheses

$$\begin{aligned} H_0(k) : & \text{The edges } E(k+h) \setminus E(k-h) \text{ are added via offset parameter } \delta. \\ H_A(k) : & \text{The edges } E(k+h) \setminus E(k) \text{ and } E(k) \setminus E(k-h) \text{ are added via} \\ & \text{offset parameters } \delta_1 \neq \delta_2. \end{aligned} \quad (15)$$

for $k = n_0 + h, \dots, n - h$. Here, $h > 0$ is chosen such that no two changepoints are within h edges of each other. In order for asymptotics developed in previous sections to kick in, h must grow with n . Henceforth, we assume $h_n = \lfloor ns \rfloor$ for some $s \in (0, 1)$. In the continuous time setting, this assume the changepoints specified under H_A in (14) are approximately separated by s for large n . With this window-based assumption, individual hypothesis tests can be performed over select windows that contain only a single changepoint, assuming a proper choice of h_n .

We slightly augment the methods of Hao et al. (2013) and Niu & Zhang (2012) for our purposes. Using likelihood ratio methods from Section 3.2, the natural statistic to test (15) is

$$\frac{L_{(k-h_n, k+h_n]}(\hat{\delta}_{(k-h_n, k+h_n]})}{L_{(k-h_n, k]}(\hat{\delta}_{(k-h_n, k]})L_{(k, k+h_n]}(\hat{\delta}_{(k, k+h_n]})} \quad \text{for } k = h_n + 1, \dots, n - h_n - 1. \quad (16)$$

Theoretically, however, this statistic is difficult to work with. Namely, if we convert to continuous time by letting $k = \lfloor nt \rfloor$, $\hat{\delta}_{(nt, n(t+s))} \approx \hat{\delta}_{(k, k+h_n)}$ and $\hat{\delta}_{(n(t-s), n(t+s))} \approx \hat{\delta}_{(k-h_n, k+h_n)}$, it is difficult to establish the joint convergence of these (scaled and centered) processes in $D[0, 1 - \gamma] \times D[\gamma, 1 - \gamma]$. In the proof of Lemma 1, we were able to get away without establishing joint convergence since $\hat{\delta}_n = \delta_{(0, n]}$ is a realization of $\delta_{(0, nt]}$ at $t = 1$. Then establishing the convergence of the scaled and centered $\delta_{(0, nt]}$ in the Skorohod space was sufficient, since the continuous mapping theorem allows us to prove statements like (1). The joint convergence of the

processes $\hat{\delta}_{(nt, n(t+s))}$ (or equivalently $\hat{\delta}_{(n(t-s), nt]}$) and $\hat{\delta}_{(n(t-s), n(t+s))}$ in (16) cannot be derived from the convergence of a single process or transformations of such processes, thus theoretical analysis becomes less tractable. We refer to Chapter 13 of Whitt (2002) for more on deriving stochastic process limits from existing ones.

Instead, we propose the statistic

$$\Lambda_k(h_n) := \frac{L_{(k-h_n, k]}(\hat{\delta}_{(k, k+h_n]}) L_{(k, k+h_n]}(\hat{\delta}_{(k-h_n, k]})}{L_{(k-h_n, k]}(\hat{\delta}_{(k-h_n, k]}) L_{(k, k+h_n]}(\hat{\delta}_{(k, k+h_n]})} \quad \text{for } k = h_n + 1, \dots, n - h_n - 1. \quad (17)$$

In the denominator (17) maximizes the likelihood under the alternative hypotheses in (15). The numerator, on the other hand, is an unsophisticated representation of the null hypothesis. Under the null, $\hat{\delta}_{(k, k+h_n]}$ and $\hat{\delta}_{(k-h_n, k]}$ should in a sense be interchangeable since they are both estimators of δ . Thus, switching the maximizers of $L_{(k-h_n, k]}(\lambda)$ and $L_{(k, k+h_n]}(\lambda)$ should result in a likelihood ratio that is approximately 1 under the null hypothesis, but far from optimal under the alternative. Note that $\hat{\delta}_{(k-h_n, k]}$ and $\hat{\delta}_{(k, k+h_n]}$ are time shifts of the same process, making continuous mapping methodology suitable for the analysis of (17).

The following corollary gives the limiting process for $-2 \log \Lambda_{[nt]}(\lfloor ns \rfloor)$. The proof is very similar to that of Theorem 1, and hence we omit it for brevity.

COROLLARY 1. *Under H_0 in (14)*

$$-2 \log \Lambda_{nt}(\lfloor ns \rfloor) \Rightarrow \frac{2}{s} (W(t+s) + W(t-s) - 2W(t))^2 \quad (18)$$

in $D[0, 1]$, where \Rightarrow denotes the weak convergence and $W(\cdot)$ is a Wiener process.

Corollary 1 provides the building block for the application of the SaRa algorithm to our PA network setup here, which we now explain.

The SaRa algorithm proceeds by collecting the locations which locally maximize $-2 \log \Lambda_k(h_n)$. Along the lines of Hao et al. (2013), we call ℓ a h -local maximizer if

$$-2 \log \Lambda_\ell(h_n) \geq -2 \log \Lambda_k(h_n), \quad \text{for all } k \in \{\ell - h, \dots, \ell + h\}.$$

For simplicity, we choose $h = h_n$ as a default, though more informed choices can be made. Naturally, these maximums locally maximize the discrepancy characterized by the likelihood ratio and provide the most evidence against the null hypothesis. Once the scanning step is complete and we have identified the h_n -local maximizers, we compare the collection of h_n -local maximums to the $(1 - \alpha)$ -th quantile of the s -local maximums of

$$X(t) := \frac{2}{s} (W(t+s) + W(t-s) - 2W(t))^2,$$

the limiting process of $-2 \log \Lambda_{[nt]}(\lfloor ns \rfloor)$. A s -local maximizer is a continuous time analog the h_n -local maximizer; t is a s -local maximizer of $X(t)$ if $X(t) \geq X(u)$ for all $u \in [t-s, t+s]$. The quantiles of the s -local maximums of $X(t)$ are difficult to obtain analytically, but since $X(t)$ is a transformation of Wiener processes, they can be easily simulated.

In comparison to (11), the statistic (17) has computational advantages. As discussed previously, the maximum likelihood estimates in (11) and (17) do not have a closed-form and are solved by setting (7) equal to zero and employing Newton's Method. In particular, for (11), one must compute the likelihood ratio at every single edge m , which further involves computing the maximum likelihood estimates $\hat{\delta}_{(0, m]}$ and $\hat{\delta}_{(m, n]}$. Even with clever programming and techniques such as warm starts, this is not easily computable for large networks. Although optimization still

needs to be performed at every time point m for (17), the window h_n also serves as a computational backstop for the procedure since optimization occurs over $2h_n$ edges rather than employing the entire edgelist. Though faster methods are still to be desired if one were to analyze large networks with other changepoint segmentation methods such as binary segmentation. We also point out that these analyses give rise to multiple hypothesis tests, so one may consider control of the false discovery rate or family wise error rate as in Hao et al. (2013). We will leave this point for future research.

4.2. Score test

Another popular way of sequentially detecting multiple changepoints is via binary segmentation Niu et al. (2016). Although there are many variants of binary segmentation, including those of Fryzlewicz (2014) and Olshen et al. (2004), we apply the routine version as presented in Algorithm 1. In the algorithm, we let $f(\cdot)$ be a function that, from an edgelist, returns TRUE if a changepoint is detected, and otherwise returns FALSE. Further, let $g(\cdot)$ be a function that returns an estimated changepoint from an edgelist.

Algorithm 1. BinarySegmentation($E(n)$, $f(\cdot)$, $g(\cdot)$)

Input: edgelist $E(n)$, $f(\cdot)$, $g(\cdot)$;
 Output: set of estimated changepoint locations $\hat{\mathcal{T}}$;
if $f(E(n))$ **then**
 $m \leftarrow g(E(n))$;
 $\hat{\mathcal{T}} \leftarrow \hat{\mathcal{T}} \cup m$;
 BinarySegmentation($E(m)$, $f(\cdot)$, $g(\cdot)$);
 BinarySegmentation($E(n) \setminus E(m)$, $f(\cdot)$, $g(\cdot)$);

Binary segmentation is a particularly convenient technique as it conveniently extends the single changepoint detection procedures to the multiple changepoint setting. Though, for computationally intensive procedures, their repeated application over multiple segments renders them infeasible for practical applications. This is especially true for dynamic networks, as the number of edges in a typical network can exceed the millions or even billions. As mentioned in Section 4.1, the likelihood ratio procedures in Section 3.2 can unfortunately become computationally onerous, which calls for the need of a quicker procedure to detect changepoints.

In order to assuage the computational bottleneck induced by the likelihood ratio methodology, we introduce a score-based statistic that drastically reduces computational load in detecting changepoints. To introduce the statistic assume for a moment that we are indeed under H_0 in (14). Under H_0 , the best estimate of δ is $\hat{\delta}_n = \hat{\delta}_{(0,n]}$, the MLE based on the entire network. By definition, $u_{(0,n]}(\hat{\delta}_n) = 0$. However, if the whole data stream is governed by $PA(\delta)$, then we might expect that $\hat{\delta}_n$ approximately solves $u_{(0,m]}(\lambda) = 0$ for any $m < n$. On the other hand, if there is a changepoint at m , $u_{(0,m]}(\hat{\delta}_n)$ should be far from 0 since $\hat{\delta}_n$ is computed under a misspecified model. This leads us to propose the following statistic for changepoint detection:

$$S_m := -u_{(0,m]}^2(\hat{\delta}_n) \left(\frac{1}{u'_{(0,m]}(\hat{\delta}_n)} + \frac{1}{u'_{(m,n]}(\hat{\delta}_n)} \right) \quad \text{for } m = \lfloor n\gamma \rfloor, \dots, \lfloor n(1-\gamma) \rfloor. \quad (19)$$

Here, we need to ensure $\lfloor n\gamma \rfloor \leq m \leq \lfloor n(1-\gamma) \rfloor$ for $\gamma \in (0, 1)$ in order to guarantee that there is sufficient data so that the score function and observed information are a good representatives of the PA process up to that point. The hessian in (19) is used as a scaling factor to eliminate

unknown parameters in the asymptotic distribution of S_m . In theory, one could employ $u'_{(0,n]}(\hat{\delta}_n)$ instead of $u'_{(0,nt]}(\hat{\delta}_n)$ for a better estimate of the asymptotic covariance of $\hat{\delta}_n$ under the null hypothesis, though we employ the latter to match the asymptotic distribution in Theorem 1. Intuitively, the likelihood ratio (11) is likely the most powerful, and hence it may be beneficial to imitate its behavior under the null hypothesis. Theorem 3 gives the asymptotic distribution of the proposed statistic under the null hypothesis, with proofs deferred to Appendix A.5. This gives rise to a hypothesis test of changepoint existence where the null hypothesis is rejected when $\sup_{t \in [\gamma, 1]} S_{nt}$ exceeds the $(1 - \alpha)$ -th quantile of a $\sup_{t \in [\gamma, 1]} B^2(t)/t(1 - t)$ distribution.

THEOREM 3. *Fix $\gamma \in (0, 1/2)$. Then under H_0 in (14)*

$$\sup_{t \in [\gamma, 1-\gamma]} S_{nt} \Rightarrow \sup_{t \in [\gamma, 1-\gamma]} \frac{B^2(t)}{t(1-t)}, \quad (20)$$

in \mathbb{R} .

By using (19), the computational load is alleviated by requiring only one computation of the MLE per segment. If (11) were applied, one would need to compute on the order of n many MLE's for the first segment. Further, since the score function is additive, it requires only $O(n)$ operations to compute S_m for $m = \lfloor n\gamma \rfloor, \dots, n$. Although we are unable to present a consistency result for the score-based method, the computational benefits are obvious.

4.3. Multiple changepoint simulation study

In this section we compare the empirical performance of the window and score methods to simulated, multiple changepoint data. As in Niu et al. (2016), it may be desirable to control the family-wise error rate (FWER) or false discovery rate (FDR) via a multiple testing procedure, though we present unadulterated results as the choice of procedure can muddy comparisons. First, we evaluate the false positive rates for the window and score methods when there is no changepoint. Since the window method finds multiple local maxima within a data sequence, we define the positive rate to be the proportion of h_n -local maximums that reject the null hypothesis out of total identified h_n -local maximums. On the other hand, the positive rate for the score test is the number of times the maximum S_m exceeds the $(1 - \alpha)$ -th quantile of the null distribution in Theorem 3 out of the number of total segments tested. Under the null, the positive rate for the score test will be close to the FWER due to the sequential nature of binary segmentation. For the window method, however, the FWER will be inflated compared to the positive rate under the null due to multiple hypothesis tests being performed at once (one for each h_n -local maxima).

To evaluate control on the false positive rate, we apply the window and score methods to 500 simulated PA(δ) networks of size 100,000 where $\delta \in \{-0.5, 0, 1, 2\}$. We let $h_n = 10,000$ for the window statistic and $\gamma = 0.1$ for the score statistic. Here, h_n and γ are chosen so that the region $[0.1, 0.9]$ is searched for a changepoint in both cases. Further, these settings are chosen to ensure that there are enough edges to accurately estimate parameters of the PA processes under each regime. The empirical false positive rate for each δ value is reported in Table 4. The false positive rates behave as expected, concentrating around $\alpha = 0.05$. The study indicates that even in the multiple changepoint setting, the hypothesis testing perspective still provides control on detecting the existence of a changepoint.

Next, we assess the ability for the window and score methods to detect multiple changepoints and estimate their locations consistently. To do so, we apply the methods to 500 simulated PA(0.2, 0.5; 1, 1.5, δ_3) networks of size 100,000. That is, the network-generating process switches from PA(1) to PA(1.5) at $t_1^* = 0.2$, and then switches from PA(1.5) to PA(δ_3)

δ	-0.5	0	1	2
Window	0.0457	0.0473	0.0556	0.0491
Score	0.0499	0.0558	0.0519	0.0519

Table 4. False positive rates for the window and score methods applied to 500 $PA(\delta)$ networks with 50,000 edges and $\gamma = 0.1$ and $h_n = 10,000$.

Method	δ_3	# of changepoints					Rand index
		0	1	2	3	4	
Window	1.0	0	12	458	29	1	0.963
	1.1	0	56	414	29	1	0.934
	1.2	3	191	282	24	0	0.851
	1.3	1	352	141	6	0	0.757
	1.4	5	425	67	3	0	0.713
Score	1.0	0	128	370	3	0	0.934
	1.1	0	36	451	13	0	0.948
	1.2	2	6	479	13	0	0.940
	1.3	0	127	363	10	0	0.858
	1.4	0	390	108	2	0	0.725

Table 5. Number of changepoints found and average rand index for the window and score methods applied to 500 $PA(0.2, 0.5; 1, 1.5, \delta_3)$ networks with 100,000 edges and $\gamma = 0.1$ and $h_n = 10,000$.

at $t_2^* = 0.5$. We allow δ_3 to vary from 1 to 1.4 by increments of 0.1. If $\delta_3 = 1$, we are under an “epidemic alternative”; the network generating process eventually returns to the state it was initialized under. As in the previous simulation, we let $h_n = 10,000$ and $\gamma = 0.1$. The estimated number of changepoints and average Rand index across the 500 simulations are reported in Table 5. For $\delta_3 = 1$, which is the largest change between the PA processes at $t^* = 0.5$, the window method exhibits the benefits of local estimation of the changepoint. Since changepoint estimation relies on local information, the initializing $PA(1)$ process does not influence the estimation. The score method performs worse in this situation since the null hypothesis estimate $\hat{\delta}_n$ reflects that the network is generating by a $PA(1)$ process for 70% of the network evolution. However, as soon as δ_3 is slightly larger than 1, the score method outperforms the window-based method. Once δ_3 becomes closer to 1.5 and the second and third PA processes become more similar, both methods exhibit poorer performance. Though, the score method more consistently detects that there are indeed 2 changepoints. Generally, the window method more accurately detects changepoints under an epidemic-like alternative, but the speed and accuracy of the score method under other settings make it a desirable choice for multiple changepoint detection.

5. DATA EXAMPLE

We now demonstrate the applicability of our changepoint detection methods to real world networks by applying our methods to the Twitter Higgs network, first analyzed in De Domenico et al. (2013) (available on Leskovec & Krevl (2014)). The Higgs boson particle, whose existence was theorized in 1964 by Peter Higgs and others, bolstered a popular theory in particle physics. On July 4th, 2012 at 8 AM GMT, scientists at CERN sent ripples through the physics community with the announcement of the discovery of a particle with properties agreeing with that of the

Higgs boson particle. Before the official announcement, however, rumors of the discovery spread through Twitter. The Twitter Higgs network tracks the activity of a subset of users discussing this discovery from July 1st to July 7th, 2012. Here, we limit our analysis to just the retweets of these users so that a directed edge (v, w) indicates that node v retweeted node w . This network is temporal, and each edge is observed in the order of its creation with a timestamp. Intuitively, one would expect that with the announcement of Higgs boson discovery, the dynamics and short term attractiveness of users retweets would shift dramatically.

Unfortunately, a retweet network is not a tree; users can retweet multiple times during the network evolution. Hence, in order to better conform with model assumptions, we remove users with out-degree larger than 1. Although this seems like a drastic adjustment, 67.6% of users retweet only once throughout the network evolution. Hence, we are still able to analyze the behavior of a typical user in the network with this data cleaning step. This resulting network contains 198,437 users.

We apply both the score and window tests to the network to detect multiple changepoints. For the score test we allow $\gamma = 0.1$, and we set $h_n = \lfloor 0.05n \rfloor = 9921$ for the window method. The score method detects 5 changepoints, while the window method detects 6. In order to correct for multiple testing, we employ a Holm adjustment to the p -values for both procedures (Holm, 1979). In this case, the Holm correction has no effect on the number of estimated changepoints, indicating the significance for the changepoints detected.

We then utilize maximum likelihood to fit preferential attachment models over the constant segments of the network defined by the changepoints. The maximum likelihood estimates and Fisher information-based confidence intervals (cf. Gao & van der Vaart (2017); Wan et al. (2017)) are given in Figures 2 and 3 for the score and window methods, respectively. Throughout, the estimated changepoints are colored in red, with the official announcement time colored in blue. Additionally, Figures 2 and 3 display the moving proportion of nodes with degrees larger than 100 within a centered time window of length 200. Note that the choice of the threshold (100, the empirical 70-percentile of the degree distribution) can be changed to any other upper quantiles of the degree distribution. Essentially, if the proportion of selected nodes with large degrees (> 100) increases within a time period, then we may expect the degree distribution to have heavier tails, and the estimated offset parameter δ over that region should decrease. As a result, the attachment mechanism has become more preferential and thus high degree nodes are more attractive.

Both methods capture the varying dynamics in users retweet behavior. The nearest changepoint to the official announcement detected by the score method was approximately two hours before the announcement at 05:49:55 GMT, while the window method produced the nearest estimated changepoint at 09:08:20 GMT on 07/04/2012. We further remark that in Figures 2 and 3, the x -axis corresponds to the number of steps in the network evolution, not the real time scale. Due to the large number of retweets produced around the announcement of the news, the first two changepoints detected by the two methods are in fact all not very far away from the official announcement in real time.

Across both methods, the proportion of attached nodes with degree greater than 100 remains relatively constant between the estimated changepoints, indicating that the attachment process has stabilized over these regions. Both methods indicate that the offset parameter δ decreases near the official announcement of the discovery, while eventually increasing towards the end of the observed network evolution. Such trend suggests that around the announcement the attachment process becomes more preferential, so that large degree nodes are more attractive over that time period. This is reasonable since initial tweets surrounding a news breaking event are likely to be popular and quickly gain attention. In later stages of the news cycle, however, the attachment

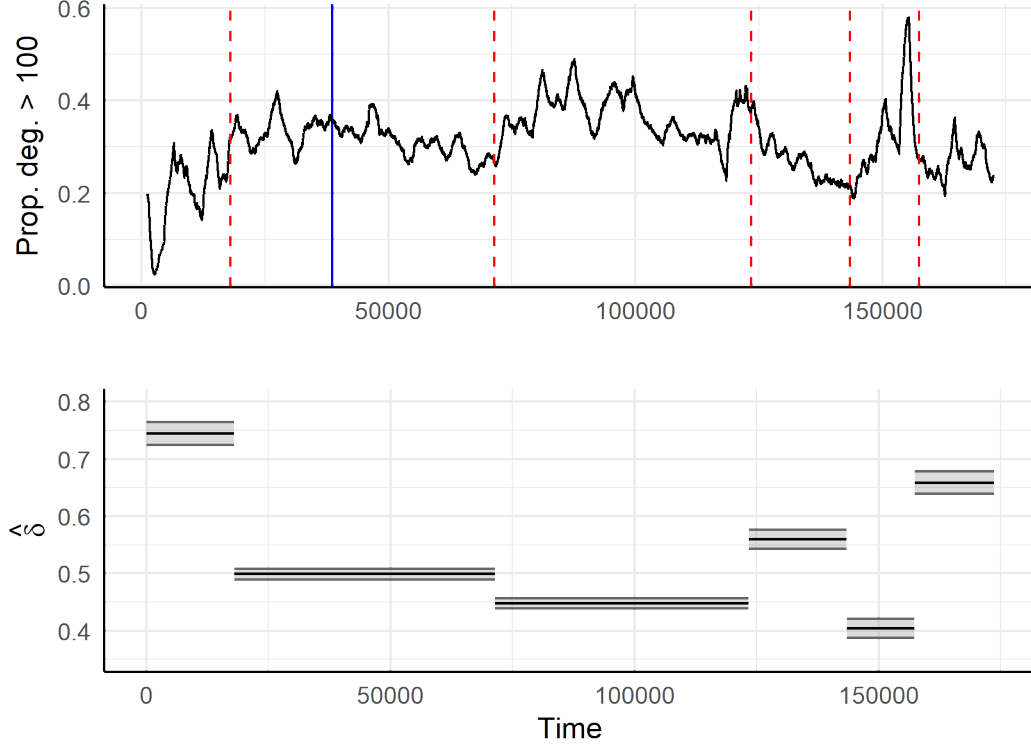


Fig. 2. Time of Higgs boson announcement (in blue) along with estimated changepoints (in red) for the score method. The first panel displays a sliding window proportion of attached nodes with degree larger than 100 over a period of length 200. The second panel displays offset parameter estimates and confidence intervals over the constant regions computed via MLE.

process becomes more uniform, indicating that attention has diffused throughout the network after a short period of time.

Although the window method is more sensitive, some estimated changepoint locations are shared across the two methods. Figure 4 reports the test statistics for the first segmentation step of the score method, as well as the likelihood ratio statistics for the window method. The lack of spikes in the score statistic between July 5th and 6th conveys the necessity of binary segmentation; without additional segmentation, the two additional changepoints in that time period would likely not have been detected. Note that for the likelihood ratio statistics, there is a later spike that remains undetected, but is classified as a changepoint via the score statistic. This spike was not classified as an h_n -local maximizer due to its proximity to another maximizer, and hence is undetected by the window method. The window h_n can be further reduced to estimate additional changepoints in the network evolution, though we choose not to do so in order to retain accurate estimation of the offset parameters.

Overall, our numerical analyses show that the preferential attachment model with changepoints, combined with our likelihood-based methodology, can be used to successfully track the dynamics of an evolving network.

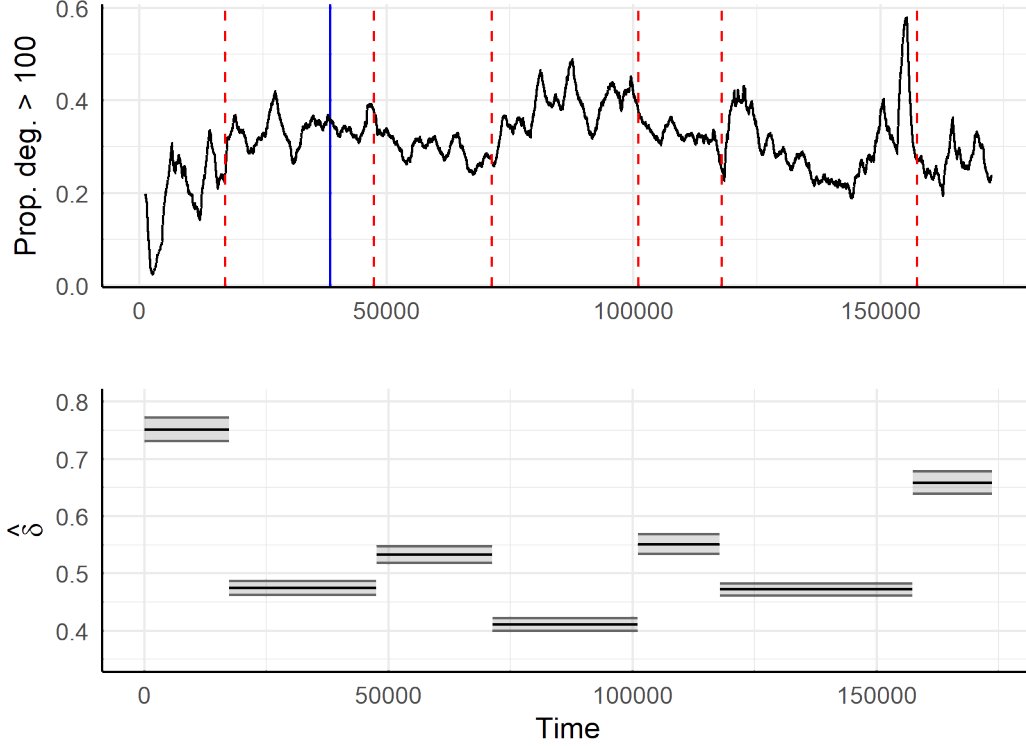


Fig. 3. Time of Higgs boson announcement (in blue) along with estimated changepoints (in red) for the window method. The first panel displays a sliding window proportion of attached nodes with degree larger than 100 over a period of length 200. The second panel displays offset parameter estimates and confidence intervals over the constant regions computed via MLE.

6. CONCLUSION

In this paper, we introduce likelihood-based methods for changepoint detection in preferential attachment models. For single changepoint detection, we produced a theoretically justified likelihood ratio test that empirically performs better than a non-parametric estimator under correctly and misspecified models. Further, we extend the likelihood based methodology to the multiple changepoint setting where both window-based and fast binary segmentation methods can be applied to large networks. The presented methods offer solutions to the statistical detection of changepoints via a hypothesis testing perspective not previously put forward in the network literature. When applied to a Twitter retweet network, the multiple changepoint methods offer a statistically sound analysis of the varying dynamics in the presence of shocks to the network evolution.

With this work, there are multiple avenues of research yet to be explored. First, one can consider the extension of these methods to more realistic network models such as the one in Wan et al. (2017). We believe the methods presented here can be extended to the case where users in a network can make multiple connections. Further, one can consider the development of likelihood-based methodology for changepoint detection in more general preferential attachment models such as sublinear preferential attachment (as in Banerjee et al. (2018); Gao et al.

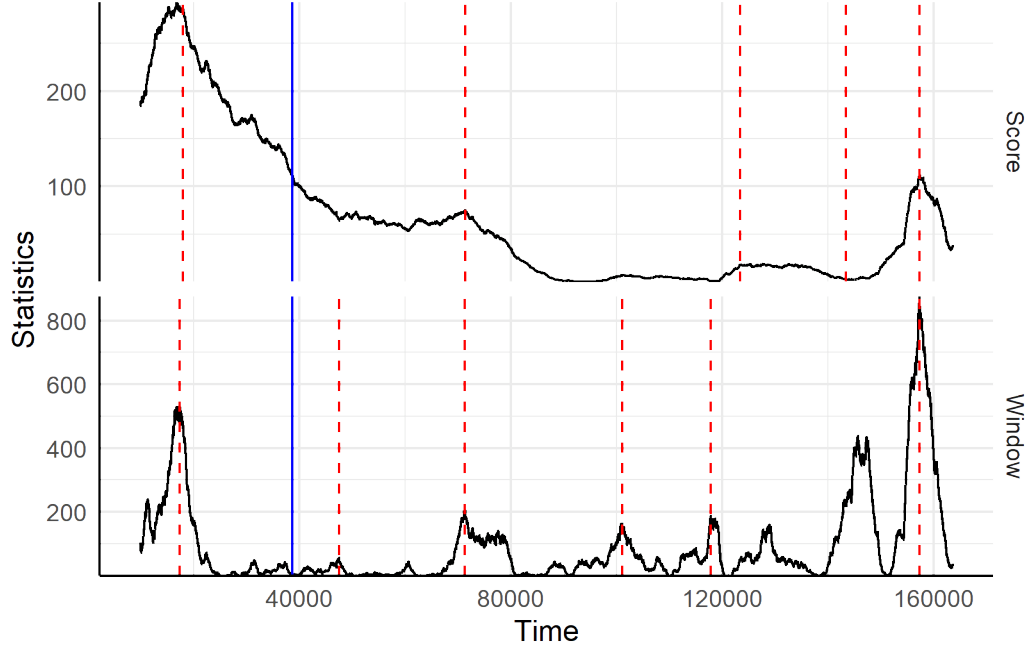


Fig. 4. The statistics S_k and $\Lambda_k(h_n)$ plotted over the network evolution along with the estimated changepoints for each method (in red). The announcement of the Higgs boson discovery is marked in blue.

(2017)). Finally, one can consider more interesting definitions of a changepoint in the network setting. Here, we considered a classical definition of changepoint where the distribution of the entire network changes, but it is also possible to assume changes in a subset of the network or some other types of changes in the network dynamics.

REFERENCES

- BANERJEE, S., BHAMIDI, S. & CARMICHAEL, I. (2018). Fluctuation bounds for continuous time branching processes and nonparametric change point detection in growing networks. *arXiv preprint arXiv:1808.02439*.
- BARABÁSI, A.-L. & ALBERT, R. (1999). Emergence of scaling in random networks. *science* **286**, 509–512.
- BHAMIDI, S., JIN, J. & NOBEL, A. (2018). Change point detection in network models: Preferential attachment and long range dependence. *The Annals of Applied Probability* **28**, 35–78.
- BOLLOBÁS, B., BORGS, C., CHAYES, J. T. & RIORDAN, O. (2003). Directed scale-free graphs. In *SODA*, vol. 3.
- CHAKRABORTY, S. & ZHANG, X. (2021). High-dimensional change-point detection using generalized homogeneity metrics. *arXiv preprint arXiv:2105.08976*.
- CIRKOVIC, D., WANG, T. & RESNICK, S. (2022). Preferential attachment with reciprocity: Properties and estimation. *arXiv preprint arXiv:2201.03769*.
- CSÖRGÖ, M., CSÖRGÖ, M. & HORVÁTH, L. (1997). Limit theorems in change-point analysis.
- DE DOMENICO, M., LIMA, A., MOUGEL, P. & MUSOLESI, M. (2013). The anatomy of a scientific rumor. *Scientific reports* **3**, 1–9.
- DURRETT, R. & RESNICK, S. I. (1978). Functional limit theorems for dependent variables. *The Annals of Probability*, 829–846.
- FRYZLEWICZ, P. (2014). Wild binary segmentation for multiple change-point detection. *The Annals of Statistics* **42**, 2243–2281.
- GAO, F. & VAN DER VAART, A. (2017). On the asymptotic normality of estimating the affine preferential attachment network models with random initial degrees. *Stochastic Processes and their Applications* **127**, 3754–3775.

- GAO, F., VAN DER VAART, A., CASTRO, R. & VAN DER HOFSTAD, R. (2017). Consistent estimation in general sublinear preferential attachment trees. *Electronic Journal of Statistics* **11**, 3979–3999.
- HAO, N., NIU, Y. S. & ZHANG, H. (2013). Multiple change-point detection via a screening and ranking algorithm. *Statistica Sinica* **23**, 1553.
- HOLM, S. (1979). A simple sequentially rejective multiple test procedure. *Scandinavian journal of statistics*, 65–70.
- KUNEGIS, J. (2013). KONECT – The Koblenz Network Collection. In *Proc. Int. Conf. on World Wide Web Companion*.
- LESKOVEC, J. & KREVL, A. (2014). SNAP Datasets: Stanford large network dataset collection. <http://snap.stanford.edu/data>.
- NIU, Y. S., HAO, N. & ZHANG, H. (2016). Multiple change-point detection: a selective overview. *Statistical Science*, 611–623.
- NIU, Y. S. & ZHANG, H. (2012). The screening and ranking algorithm to detect dna copy number variations. *The annals of applied statistics* **6**, 1306.
- OLSHEN, A. B., VENKATRAMAN, E., LUCITO, R. & WIGLER, M. (2004). Circular binary segmentation for the analysis of array-based dna copy number data. *Biostatistics* **5**, 557–572.
- VAN DER HOFSTAD, R. (2017). *Random graphs and complex networks*, vol. 43. Cambridge university press.
- WAN, P., WANG, T., DAVIS, R. A. & RESNICK, S. I. (2017). Fitting the linear preferential attachment model. *Electronic Journal of Statistics* **11**, 3738–3780.
- WANG, T. & RESNICK, S. I. (2020). A directed preferential attachment model with poisson measurement. *arXiv preprint arXiv:2008.07005*.
- WHITT, W. (2002). Stochastic-process limits: an introduction to stochastic-process limits and their application to queues. *Space* **500**, 391–426.

A. PROOFS

A.1. Proof of Theorem 1

The proof of Theorem 1 requires the weak convergence of $\sqrt{n}(\hat{\delta}_{(ns, nt]} - \delta)$, which is given in Lemma 1. The weak convergence of $\sqrt{n}(\hat{\delta}_{(ns, nt]} - \delta)$ further relies on the weak convergence of the score function evaluated at the truth, $n^{-1}u_{(0, nt]}(\delta)$, to a Wiener process. To prove this, we rely on the fact that the summands of $n^{-1}u_{(0, nt]}(\delta)$ are a martingale difference array, and hence we can apply functional martingale central limit theorems (FMCLT). We now present Lemma 1.

LEMMA 1. Fix $s \in [0, 1]$ and $\tau \in (0, 1 - s)$. Assume that edges $[ns] + 1$ to $[nt]$, $s + \tau \leq t \leq 1$ are added according to the PA(δ) rule. Then as $n \rightarrow \infty$

$$(t - s)I(\delta) \cdot \sqrt{n}(\hat{\delta}_{(ns, nt]} - \delta) \Rightarrow W(tI(\delta)) - W(sI(\delta))$$

in $D[s + \tau, 1]$ where $W(\cdot)$ is a Wiener process, and

$$I(\lambda) = \sum_{i=1}^{\infty} \frac{p_{>i}(\delta)}{(i + \lambda)^2} - \frac{1}{(2 + \lambda)^2},$$

for $\lambda \in [\eta, K]$.

We defer the proof of Lemma 1 to Section A.2, and proceed with the proof of Theorem 1.

Proof. From (11), we see that

$$\begin{aligned} -2 \log \Lambda_{nt} &= \left(2\ell_{(0, nt]}(\hat{\delta}_{(0, nt]}) - 2\ell_{(0, nt]}(\hat{\delta}_n) \right) + \left(2\ell_{(nt, n]}(\hat{\delta}_{(nt, n]}) - 2\ell_{(nt, n]}(\hat{\delta}_n) \right) \\ &:= I_{(0, nt]} + I_{(nt, n]}. \end{aligned}$$

We first focus on $I_{(0,nt]}$. Applying Taylor's expansion to $\ell_{(0,nt]}(\cdot)$, we have that there exists δ_n^* between $\hat{\delta}_{(0,nt]}$ and $\hat{\delta}_n$ such that

$$\begin{aligned}\ell_{(0,nt]}(\hat{\delta}_n) - \ell_{(0,nt]}(\hat{\delta}_{(0,nt]}) &= u_{(0,nt]}(\hat{\delta}_{(0,nt]}) \left(\hat{\delta}_n - \hat{\delta}_{(0,nt]} \right) + \frac{u'_{(0,nt]}(\delta_n^*)}{2} \left(\hat{\delta}_n - \hat{\delta}_{(0,nt]} \right)^2 \\ &= \frac{u'_{(0,nt]}(\delta_n^*)}{2} \left(\hat{\delta}_n - \hat{\delta}_{(0,nt]} \right)^2.\end{aligned}$$

Therefore,

$$I_{(0,nt]} = -u'_{(0,nt]}(\delta_n^*) \left(\hat{\delta}_n - \hat{\delta}_{(0,nt]} \right)^2 = -\frac{1}{n} u'_{(0,nt]}(\delta_n^*) \left(\sqrt{n} \left(\hat{\delta}_n - \hat{\delta}_{(0,nt]} \right) \right)^2.$$

Also, since

$$\sqrt{n} \left(\hat{\delta}_n - \hat{\delta}_{(0,nt]} \right) = \sqrt{n} \left(\hat{\delta}_n - \delta \right) - \sqrt{n} \left(\hat{\delta}_{(0,nt]} - \delta \right), \quad (1)$$

and by Lemma 1 as well as the continuity of the functional $F : x \in D[\gamma, 1] \mapsto x(1) - x$, we have

$$tI(\delta) \cdot \sqrt{n} \left(\hat{\delta}_n - \hat{\delta}_{(0,nt]} \right) \Rightarrow tW(I(\delta)) - W(tI(\delta)) \quad \text{in } D[\gamma, 1]. \quad (2)$$

Similar arguments as in (ii) and (iii) in the proof of Lemma 1 give that

$$tI(\delta) \cdot I_{(0,nt]} \Rightarrow (W(tI(\delta)) - tW(I(\delta)))^2, \quad \text{in } D[\gamma, 1].$$

Defining the Brownian bridge $B(t) := I^{-1/2}(\delta) (W(tI(\delta)) - tW(I(\delta)))$, we thus have

$$I_{(0,nt]} \Rightarrow \frac{B^2(t)}{t}, \quad \text{in } D[\gamma, 1].$$

Nearly the same proof methodology applies for $I_{(nt,n]}$, thus giving that

$$I_{(nt,n]} \Rightarrow \frac{B^2(t)}{1-t} \quad \text{in } D[0, 1-\gamma]. \quad (3)$$

Applying the continuity of the functional $G : x(t) \in D[\gamma, 1-\gamma] \mapsto x(t) + x(1-t)$ we thus have that $I_{(0,nt]} + I_{(nt,n]}$ converges weakly to the sum of their respective limits, which can be rewritten as

$$\frac{B^2(t)}{t} + \frac{B^2(t)}{1-t} = \frac{B^2(t)}{t(1-t)},$$

Thus

$$-2 \log \Lambda_{nt} \Rightarrow \frac{B^2(t)}{t(1-t)}, \quad \text{in } D[\gamma, 1-\gamma]. \quad (4)$$

Finally, using continuity of the functional

$$G : x \in D[\gamma, 1-\gamma] \mapsto \sup_{t \in [\gamma, 1-\gamma]} x(t),$$

we have that

$$\sup_{t \in [\gamma, 1-\gamma]} -2 \log \Lambda_{nt} \Rightarrow \sup_{t \in [\gamma, 1-\gamma]} \frac{B^2(t)}{t(1-t)} \quad \text{in } \mathbb{R}.$$

A.2. Proof of Lemma 1

In the spirit of Wan et al. (2017), we use Taylor expansion to rewrite the score at $\hat{\delta}_{(ns,nt]}$ around δ . Then

$$0 = u_{(ns,nt]}(\delta) + u'_{(ns,nt]}(\delta_n^*) (\hat{\delta}_{(ns,nt]} - \delta), \quad (5)$$

where $\delta_n^* = \delta + \xi(\hat{\delta}_{(ns,nt]} - \delta)$ for some $\xi \in [0, 1]$. The intermediate value δ_n^* depends on t , though we drop this dependence in notation. Some algebra then gives

$$\sqrt{n}(\hat{\delta}_{(ns,nt]} - \delta) = - \left(\frac{1}{\frac{1}{n}u'_{(ns,nt]}(\delta_n^*)} \right) n^{-1/2}u_{(ns,nt]}(\delta). \quad (6)$$

The following results are used to prove Lemma 1:

- (i) $n^{-1/2}u_{(0,nt]}(\delta) \Rightarrow W(tI(\delta))$ in $D[0, 1]$,
- (ii) $\sup_{t \in [0,1]} \sup_{\lambda \in [\eta, K]} \left| -n^{-1}u'_{(0,nt]}(\lambda) - tI(\lambda) \right| \xrightarrow{P} 0$,
- (iii) $\sup_{t \in [s+\tau, 1]} \left| \hat{\delta}_{(ns,nt]} - \delta \right| \xrightarrow{P} 0$.

where $W(\cdot)$ is a Wiener process on $[0, 1]$. The use of τ in (iii) ensures that t is not chosen to be exactly s , and retains compactness of the index set. We prove these results in Lemmas 2, 3 and 4, respectively. Lemma 2 combined with the continuity of the functional $F : x \in D[s + \tau, 1] \mapsto x - x(s)$ gives that

$$n^{-1/2}u_{(ns,nt]}(\delta) = n^{-1/2}u_{(0,nt]}(\delta) - n^{-1/2}u_{(0,ns]}(\delta) \Rightarrow W(tI(\delta)) - W(sI(\delta)), \quad (7)$$

in $D[s + \tau, 1]$. Lemma 3 gives that

$$\begin{aligned} & \sup_{t \in [s+\tau, 1]} \sup_{\lambda \in [\eta, K]} \left| -n^{-1}u'_{(ns,nt]}(\lambda) - (t-s)I(\lambda) \right| \\ &= \sup_{t \in [s+\tau, 1]} \sup_{\lambda \in [\eta, K]} \left| -n^{-1}u'_{(0,nt]}(\lambda) + n^{-1}u'_{(0,ns]}(\lambda) - tI(\lambda) + sI(\lambda) \right| \\ &\leq \sup_{t \in [s+\tau, 1]} \sup_{\lambda \in [\eta, K]} \left| -n^{-1}u'_{(0,nt]}(\lambda) - tI(\lambda) \right| + \sup_{\lambda \in [\eta, K]} \left| n^{-1}u'_{(0,ns]}(\lambda) + sI(\lambda) \right| \xrightarrow{P} 0. \end{aligned}$$

We now establish the convergence $-n^{-1}u'_{(ns,nt]}(\delta_n^*) \xrightarrow{P} (t-s)I(\delta)$ in $D[s + \tau, 1]$. See that

$$\begin{aligned} & \sup_{t \in [s+\tau, 1]} \left| -n^{-1}u'_{(ns,nt]}(\delta_n^*) - (t-s)I(\delta) \right| \\ &\leq \sup_{t \in [s+\tau, 1]} \left| -n^{-1}u'_{(ns,nt]}(\delta_n^*) - (t-s)I(\delta_n^*) \right| + \sup_{t \in [s+\tau, 1]} |(t-s)I(\delta_n^*) - (t-s)I(\delta)| \quad (8) \\ &\leq \sup_{t \in [s+\tau, 1]} \sup_{\lambda \in [\eta, K]} \left| -n^{-1}u'_{(ns,nt]}(\lambda) - (t-s)I(\lambda) \right| + (1-s) \sup_{t \in [s+\tau, 1]} |I(\delta_n^*) - I(\delta)|. \end{aligned}$$

The first term converges in probability to 0. Since $I(\lambda)$ is (uniformly) continuous on $[\eta, K]$, it suffices to show that $\delta_n^* \xrightarrow{P} \delta$ in $D[s + \tau, 1]$. Since $|\delta_n^* - \delta| \leq |\hat{\delta}_{(ns,nt]} - \delta|$, we can instead show that $\sup_{t \in [s+\tau, 1]} |\hat{\delta}_{(ns,nt]} - \delta| \xrightarrow{P} 0$. This is proven in Lemma 4.

Thus, $\sup_{t \in [s+\tau, 1]} |I(\delta_n^*) - I(\delta)| \xrightarrow{P} 0$. Hence, by (8)

$$-n^{-1}u'_{(ns,nt]}(\delta_n^*) \xrightarrow{P} (t-s)I(\delta) \quad \text{in } D[s + \tau, 1]. \quad (9)$$

Combining the convergences (7) and (9), we have that jointly in $D[s + \tau, 1] \times D[s + \tau, 1]$

$$\begin{pmatrix} n^{-1/2}u_{(ns,nt]}(\delta) \\ -n^{-1}u'_{(ns,nt]}(\delta_n^*) \end{pmatrix} \Rightarrow \begin{pmatrix} W(tI(\delta)) - W(sI(\delta)) \\ (t-s)I(\delta) \end{pmatrix}.$$

Finally, by one last application of the continuous mapping theorem

$$(t-s)I(\delta) \cdot \sqrt{n}(\hat{\delta}_{(ns,nt]} - \delta) = - \frac{(t-s)I(\delta)}{\frac{1}{n}u'_{(ns,nt]}(\delta_n^*)} n^{-1/2}u_{(ns,nt]}(\delta) \Rightarrow W(tI(\delta)) - W(sI(\delta)).$$

A.3. Supporting Lemmas for the Proof of Lemma 1

LEMMA 2. As $n \rightarrow \infty$,

$$n^{-1/2}u_{(0,nt]}(\delta) \Rightarrow W(tI(\delta)),$$

in $D[0, 1]$.

Proof. We look to apply Theorem 2.3 in Durrett & Resnick (1978), which we record as Theorem 4 for convenience. Towards this end, define

$$\eta_{n,k} = \frac{1}{\sqrt{n}} \left(\frac{1}{D_{v_k}(k-1) + \delta} - \frac{1}{2 + \delta} \right), \quad (10)$$

and let $\mathcal{F}_{n,k} = \sigma(G(0), G(1), \dots, G(k))$. $\eta_{n,k}$ is a martingale difference array since

$$\begin{aligned} \mathbb{E}[\eta_{n,k} \mid \mathcal{F}_{n,k}] &= \frac{1}{\sqrt{n}} \left(\sum_{w=1}^{k-1} \frac{1}{D_w(k-1) + \delta} \frac{D_w(k-1) + \delta}{(k-1)(2 + \delta)} - \frac{1}{2 + \delta} \right) \\ &= \frac{1}{\sqrt{n}} \left(\sum_{w=1}^{k-1} \frac{1}{(k-1)(2 + \delta)} - \frac{1}{2 + \delta} \right) = 0. \end{aligned}$$

To show convergence, we confirm (a) of Theorem 4. Note that

$$\begin{aligned} &\sum_{k=3}^{\lfloor nt \rfloor} \mathbb{E}[\eta_{n,k}^2 \mid \mathcal{F}_{n,k}] \\ &= \frac{1}{n} \sum_{k=3}^{\lfloor nt \rfloor} \mathbb{E} \left[\frac{1}{D_{v_k}(k-1) + \delta} \left(\frac{1}{D_{v_k}(k-1) + \delta} - \frac{1}{2 + \delta} \right) \right. \\ &\quad \left. - \frac{1}{2 + \delta} \left(\frac{1}{D_{v_k}(k-1) + \delta} - \frac{1}{2 + \delta} \right) \mid \mathcal{F}_{n,k} \right]. \end{aligned}$$

The right hand term is 0 by a similar computation as before. Continuing with the remaining term, we have

$$\begin{aligned} &\frac{1}{n} \sum_{k=3}^{\lfloor nt \rfloor} \mathbb{E} \left[\frac{1}{D_{v_k}(k-1) + \delta} \left(\frac{1}{D_{v_k}(k-1) + \delta} - \frac{1}{2 + \delta} \right) \mid \mathcal{F}_{n,k} \right] \\ &= \frac{1}{n} \sum_{k=3}^{\lfloor nt \rfloor} \mathbb{E} \left[\frac{1}{(D_{v_k}(k-1) + \delta)^2} - \frac{1}{2 + \delta} \frac{1}{D_{v_k}(k-1) + \delta} \mid \mathcal{F}_{n,k} \right] \\ &= \frac{1}{n} \sum_{k=3}^{\lfloor nt \rfloor} \sum_{w=1}^{k-1} \frac{1}{(D_w(k-1) + \delta)^2} \frac{D_w(k-1) + \delta}{(k-1)(2 + \delta)} - \frac{1}{2 + \delta} \frac{1}{n} \sum_{k=3}^{\lfloor nt \rfloor} \sum_{w=1}^{k-1} \frac{1}{D_w(k-1) + \delta} \frac{D_w(k-1) + \delta}{(k-1)(2 + \delta)} \\ &= \frac{1}{2 + \delta} \frac{1}{n} \sum_{k=3}^{\lfloor nt \rfloor} \frac{1}{k-1} \sum_{w=1}^{k-1} \frac{1}{D_w(k-1) + \delta} - \frac{1}{2 + \delta} \frac{1}{n} \sum_{k=3}^{\lfloor nt \rfloor} \frac{1}{2 + \delta} \\ &= \frac{1}{2 + \delta} \frac{1}{n} \sum_{k=3}^{\lfloor nt \rfloor} \frac{1}{k-1} \sum_{w=1}^{k-1} \sum_{i=1}^{\infty} \frac{1_{\{D_w(k-1)=i\}}}{i + \delta} - \frac{\lfloor nt \rfloor - 2}{n} \frac{1}{(2 + \delta)^2} \\ &= \frac{1}{2 + \delta} \frac{1}{n} \sum_{k=3}^{\lfloor nt \rfloor} \sum_{i=1}^{\infty} \frac{N_i(k-1)/(k-1)}{i + \delta} - \frac{\lfloor nt \rfloor - 2}{n} \frac{1}{(2 + \delta)^2} \\ &= \frac{t}{2 + \delta} \frac{1}{nt} \sum_{k=3}^{\lfloor nt \rfloor} \sum_{i=1}^{\infty} \frac{N_i(k-1)/(k-1)}{i + \delta} - \frac{\lfloor nt \rfloor - 2}{n} \frac{1}{(2 + \delta)^2}. \end{aligned}$$

Since $N_i(n)/n \xrightarrow{a.s.} p_i(\delta)$ by (2), Cesàro convergence of random variables gives that $\frac{1}{nt} \sum_{k=1}^{\lfloor nt \rfloor} \sum_{i=1}^{\infty} \frac{N_i(k-1)/(k-1)}{i+\delta} \xrightarrow{a.s.} \sum_{i=1}^{\infty} \frac{p_i(\delta)}{i+\delta} = \frac{1}{2+\delta} \sum_{i=1}^{\infty} \frac{p_{>i}(\delta)}{(i+\delta)^2}$. Thus

$$\sum_{k=3}^{\lfloor nt \rfloor} \mathbb{E} [\eta_{n,k}^2 \mid \mathcal{F}_{n,k}] \xrightarrow{p} t \left(\sum_{i=1}^{\infty} \frac{p_{>i}(\delta)}{(i+\delta)^2} - \frac{1}{(2+\delta)^2} \right) = tI(\delta). \quad (11)$$

Next we confirm (b) of Theorem 4. Fix $\epsilon > 0$ and note that

$$\left| \frac{1}{D_{v_k}(k-1)+\delta} - \frac{1}{2+\delta} \right| \leq \left| \frac{1}{D_{v_k}(k-1)+\delta} \right| + \left| \frac{1}{2+\delta} \right| \leq \frac{1}{1+\delta} + \frac{1}{2+\delta} := m(\delta). \quad (12)$$

Hence, $|\eta_{n,k}| \leq \frac{1}{\sqrt{n}} m(\delta)$. Thus

$$\sum_{k=3}^{\lfloor nt \rfloor} \mathbb{E} [\eta_{n,k}^2 1_{\{|\eta_{n,k}| > \epsilon\}} \mid \mathcal{F}_{n,k}] \leq m^2(\delta) \frac{1}{n} \sum_{k=3}^{\lfloor nt \rfloor} \mathbb{P} (|\eta_{n,k}| > \epsilon \mid \mathcal{F}_{n,k}).$$

Since $\mathbb{P} (|\eta_{n,k}| > \epsilon \mid \mathcal{F}_{n,k}) \xrightarrow{a.s.} 0$, Cesàro convergence thus gives that the bound tends to 0 almost surely and $\sum_{k=3}^{\lfloor nt \rfloor} \mathbb{E} [\eta_{n,k}^2 1_{\{|\eta_{n,k}| > \epsilon\}} \mid \mathcal{F}_{n,k}] \xrightarrow{a.s.} 0$. Since all conditions are satisfied, Theorem 2.3 gives

$$n^{-1/2} u_{(0,nt]}(\delta) = \frac{1}{\sqrt{n}} \sum_{k=3}^{\lfloor nt \rfloor} \left(\frac{1}{D_{v_k}(k-1)+\delta} - \frac{1}{2+\delta} \right) \Rightarrow W(tI(\delta)) \text{ in } D[0,1]. \quad (13)$$

THEOREM 4. Suppose $\{X_{n,i}, \mathcal{F}_{n,i}\}$ is a martingale difference array where $\mathcal{F}_{n,i}$ is sequence of sigma algebras that increase with n . If

- (a) for all $t \in [0,1]$, $\sum_{i=1}^{\lfloor nt \rfloor} \mathbb{E} [X_{n,i} \mid \mathcal{F}_{n,i}] \xrightarrow{p} ct$ for some $c > 0$ and
- (b) for all $\epsilon > 0$, $\sum_{i=1}^{\lfloor nt \rfloor} \mathbb{E} [X_{n,i}^2 1_{\{|X_{n,i}| > \epsilon\}} \mid \mathcal{F}_{n,i}] \xrightarrow{p} 0$

then $\sum_{i=1}^{\lfloor nt \rfloor} X_{n,i} \Rightarrow W(ct)$ in $D[0,1]$, where $W(\cdot)$ is a Wiener process.

LEMMA 3. As $n \rightarrow \infty$,

$$\sup_{t \in [0,1]} \sup_{\lambda \in [\eta, K]} |n^{-1} u_{(0,nt]}(\lambda) - tU(\lambda)| \xrightarrow{p} 0,$$

and

$$\sup_{t \in [0,1]} \sup_{\lambda \in [\eta, K]} |-n^{-1} u'_{(0,nt]}(\lambda) - tI(\lambda)| \xrightarrow{p} 0,$$

where

$$U(\lambda) = \sum_{i=1}^{\infty} \frac{p_{>i}(\delta)}{i+\lambda} - \frac{1}{2+\lambda}.$$

Proof. We only prove the second result, as the proof for the first is nearly identical. The proof follows those of Gao & van der Vaart (2017) and Wan et al. (2017), with minor adjustments for the supremum

norm in t . First, see that by using a similar strategy as in Lemma 2

$$\begin{aligned}
-\frac{1}{n}u'_{(0,nt]}(\lambda) &= \frac{1}{n} \sum_{k=3}^{\lfloor nt \rfloor} \frac{1}{(D_{v_k}(k-1) + \lambda)^2} - \frac{\lfloor nt \rfloor - 2}{n(2 + \lambda)^2} \\
&= \frac{1}{n} \sum_{k=3}^{\lfloor nt \rfloor} \sum_{i=1}^{\infty} \frac{1_{\{D_{v_k}(k-1)=i\}}}{(i + \lambda)^2} - \frac{\lfloor nt \rfloor - 2}{n(2 + \lambda)^2} \\
&= \sum_{i=1}^{\infty} \frac{N_{>i}(\lfloor nt \rfloor)/n}{(i + \lambda)^2} - \frac{1}{n} \sum_{i=1}^{\infty} \frac{21_{\{i=1\}}}{(i + \lambda)^2} - \frac{\lfloor nt \rfloor - 2}{n(2 + \lambda)^2} \\
&= \sum_{i=1}^{\infty} \frac{N_{>i}(\lfloor nt \rfloor)/n}{(i + \lambda)^2} - \frac{1}{n} \frac{2}{(1 + \lambda)^2} - \frac{\lfloor nt \rfloor - 2}{n(2 + \lambda)^2}.
\end{aligned}$$

Further,

$$\begin{aligned}
&\sup_{t \in [0,1]} \sup_{\lambda \in [\eta, K]} \left| -n^{-1}u'_{(0,nt]}(\lambda) - tI(\lambda) \right| \\
&\leq \sup_{t \in [0,1]} \sup_{\lambda \in [\eta, K]} \left| \sum_{i=1}^{\infty} \frac{N_{>i}(\lfloor nt \rfloor)/n}{(i + \lambda)^2} - \sum_{i=1}^{\infty} \frac{p_{>i}(\delta)}{(i + \lambda)^2} \right| + \frac{1}{n} \frac{2}{(1 + \eta)^2} \\
&\quad + \sup_{t \in [0,1]} \sup_{\lambda \in [\eta, K]} \left| -\frac{\lfloor nt \rfloor - 2}{n(2 + \lambda)^2} + \frac{1}{(2 + \lambda)^2} \right|.
\end{aligned}$$

Clearly, the second term converges to 0. The third term also converges to 0 since

$$\sup_{t \in [0,1]} \sup_{\lambda \in [\eta, K]} \left| -\frac{\lfloor nt \rfloor - 2}{n(2 + \lambda)^2} + \frac{1}{(2 + \lambda)^2} \right| \leq \frac{1}{(2 + \eta)^2} \sup_{t \in [0,1]} \left| -\frac{\lfloor nt \rfloor - 2}{n} + 1 \right| \rightarrow 0.$$

We now turn our attention to the first term. From (3), we have that $N_{>i}(\lfloor nt \rfloor)/n \xrightarrow{p} tp_{>i}(\delta)$ for any $t \in [0, 1]$. Since $N_{>i}(\lfloor nt \rfloor)/n$ is a monotone and $tp_{>i}(\delta)$ is continuous as functions of t , this convergence is uniform, i.e.

$$\sup_{t \in [0,1]} |N_{>i}(\lfloor nt \rfloor)/n - tp_{>i}(\delta)| \xrightarrow{p} 0. \tag{14}$$

Also note that for every $i \geq 1$

$$iN_{>i}(\lfloor nt \rfloor) = i \sum_{j=i+1}^{\infty} N_j(\lfloor nt \rfloor) \leq \sum_{j=1}^{\infty} jN_j(\lfloor nt \rfloor) = 2\lfloor nt \rfloor,$$

since summing over the degrees returns twice the number of edges. Hence

$$N_{>i}(\lfloor nt \rfloor)/nt \leq N_{>i}(\lfloor nt \rfloor)/\lfloor nt \rfloor \leq 2/i.$$

We thus have for any $M \in \mathbb{N}$

$$\begin{aligned}
&\sup_{t \in [0,1]} \sup_{\lambda \in [\eta, K]} \left| \sum_{i=1}^{\infty} \frac{N_{>i}(\lfloor nt \rfloor)/n}{(i + \lambda)^2} - \sum_{i=1}^{\infty} \frac{p_{>i}(\delta)}{(i + \lambda)^2} \right| \\
&\leq \sum_{i=1}^{\infty} \frac{\sup_{t \in [0,1]} |N_{>i}(\lfloor nt \rfloor)/n - tp_{>i}(\delta)|}{(i + \eta)^2} \\
&\leq \sum_{i=1}^M \frac{\sup_{t \in [0,1]} |N_{>i}(\lfloor nt \rfloor)/n - tp_{>i}(\delta)|}{(i + \eta)^2} + \sum_{i=M+1}^{\infty} \frac{2/i}{(i + \eta)^2} + \sum_{i=M+1}^{\infty} \frac{p_{>i}(\delta)}{(i + \eta)^2}.
\end{aligned}$$

By choosing large enough M , the last two terms can be made arbitrarily small. By (14), the first term converges in probability to 0. Putting these results together, we have

$$\sup_{t \in [0,1]} \sup_{\lambda \in [\eta, K]} \left| -n^{-1} u'_{(0,nt]}(\lambda) - tI(\lambda) \right| \xrightarrow{P} 0.$$

LEMMA 4. Fix $s \in [0, 1]$ and $\tau \in (0, 1 - s)$. Assume that edges $[ns] + 1$ to $[nt]$, $s + \tau \leq t \leq 1$ are added according to the $PA(\delta)$ rule. Then as $n \rightarrow \infty$

$$\sup_{t \in [s+\tau, 1]} \left| \hat{\delta}_{(ns, nt]} - \delta \right| \xrightarrow{P} 0.$$

Proof. This proof closely follows that of Theorem 3.2 in Wan et al. (2017). From Lemma 4 of Gao & van der Vaart (2017), $U(\lambda)$ has a unique zero at $\lambda = \delta$. Furthermore, it is positive for $\lambda < \delta$ and negative for $\lambda > \delta$.

Fix $\epsilon > 0$. By continuity of $U(\lambda)$, there exists $\xi > 0$ such that $U(\lambda) > \epsilon/\tau$ on $[\eta, \delta - \xi]$ and $U(\lambda) < -\epsilon/\tau$ on $[\delta + \xi, K]$. Hence

$$\inf_{\lambda \in [\eta, \delta - \xi]} \inf_{t \in [s+\tau, 1]} (t - s)U(\lambda) > \epsilon \quad \text{and} \quad \sup_{\lambda \in [\delta + \xi, K]} \sup_{t \in [s+\tau, 1]} (t - s)U(\lambda) < -\epsilon.$$

Further, for all $\lambda \in [\eta, \delta - \xi]$ and $t \in [s + \tau, 1]$,

$$\begin{aligned} n^{-1} u_{(ns, nt]}(\lambda) &\geq (t - s)U(\lambda) - \sup_{v \in [s+\tau, 1]} \sup_{\lambda \in [\eta, K]} |n^{-1} u_{(ns, nv]}(\lambda) - (v - s)U(\lambda)| \\ &> \epsilon - \sup_{v \in [s+\tau, 1]} \sup_{\lambda \in [\eta, K]} |n^{-1} u_{(ns, nv]}(\lambda) - (v - s)U(\lambda)|. \end{aligned}$$

Similarly, for all $\lambda \in [\delta + \xi, K]$ and $t \in [s + \tau, 1]$,

$$\begin{aligned} n^{-1} u_{(ns, nt]}(\lambda) &\leq (t - s)U(\lambda) + \sup_{v \in [s+\tau, 1]} \sup_{\lambda \in [\eta, K]} |n^{-1} u_{(ns, nv]}(\lambda) - (v - s)U(\lambda)| \\ &< -\epsilon + \sup_{v \in [s+\tau, 1]} \sup_{\lambda \in [\eta, K]} |n^{-1} u_{(ns, nv]}(\lambda) - (v - s)U(\lambda)|. \end{aligned}$$

By Lemma 3, we see that

$$\mathbb{P} \left(\sup_{v \in [s+\tau, 1]} \sup_{\lambda \in [\eta, K]} |n^{-1} u_{(ns, nv]}(\lambda) - (v - s)U(\lambda)| < \epsilon/2 \right) \rightarrow 1 \quad \text{as } n \rightarrow \infty.$$

Hence with probability tending towards 1 as $n \rightarrow \infty$

$$\inf_{t \in [s+\tau, 1]} \inf_{\lambda \in [\eta, \delta - \xi]} n^{-1} u_{(ns, nt]}(\lambda) \geq \epsilon/2 \quad \text{and} \quad \sup_{t \in [s+\tau, 1]} \sup_{\lambda \in [\delta + \xi, K]} n^{-1} u_{(ns, nt]}(\lambda) \leq -\epsilon/2.$$

Since $u_{(ns, nt]}(\hat{\delta}_{(ns, nt]}) = 0 \forall t \in [s + \tau, 1]$, this implies

$$\mathbb{P} \left(\sup_{t \in [s+\tau, 1]} \left| \hat{\delta}_{(ns, nt]} - \delta \right| < \xi \right) \rightarrow 1.$$

A.4. Proof of Theorem 2

To prove (13), we show that for any $\tau > 0$ and for some $\kappa > 0$

$$\mathbb{P}(-2 \log \Lambda_{nt^*} > \sup_{s \in [\gamma, t^* - \tau]} -2 \log \Lambda_{ns} + \kappa) \rightarrow 1, \quad \text{as } n \rightarrow \infty. \quad (15)$$

The proof for $s \in [t^* + \tau, 1 - \gamma]$ is similar and hence we omit it. Akin to the proof of Theorem 1, we write

$$\begin{aligned} & -2 \log \Lambda_{nt^*} + 2 \log \Lambda_{ns} \\ & = 2\ell_{(0,nt^*]}(\hat{\delta}_{(0,nt^*]}) + 2\ell_{(nt^*,n]}(\hat{\delta}_{(nt^*,n]}) - 2\ell_{(0,ns]}(\hat{\delta}_{(0,ns]}) - 2\ell_{(ns,n]}(\hat{\delta}_{(ns,n]}), \end{aligned}$$

and since $\ell_{(ns,n]}(\hat{\delta}_{(ns,n]}) = \ell_{(ns,nt^*]}(\hat{\delta}_{(ns,n]}) + \ell_{(nt^*,n]}(\hat{\delta}_{(ns,n]})$, and $\ell_{(0,nt^*]}(\hat{\delta}_{(0,nt^*]}) = \ell_{(0,ns]}(\hat{\delta}_{(0,nt^*]}) + \ell_{(ns,nt^*]}(\hat{\delta}_{(0,nt^*]})$, we have

$$\begin{aligned} & = 2 \left(\ell_{(0,ns]}(\hat{\delta}_{(0,nt^*]}) - \ell_{(0,ns]}(\hat{\delta}_{(0,ns]}) \right) + 2 \left(\ell_{(ns,nt^*]}(\hat{\delta}_{(0,nt^*]}) - \ell_{(ns,nt^*]}(\hat{\delta}_{(ns,n]}) \right) \\ & \quad + 2 \left(\ell_{(nt^*,n]}(\hat{\delta}_{(nt^*,n]}) - \ell_{(nt^*,n]}(\hat{\delta}_{(ns,n]}) \right) \\ & = 2 \left(\ell_{(0,ns]}(\hat{\delta}_{(0,nt^*]}) - \ell_{(0,ns]}(\hat{\delta}_{(0,ns]}) \right) + 2 \left(\ell_{(ns,nt^*]}(\hat{\delta}_{(ns,nt^*]}) - \ell_{(ns,nt^*]}(\hat{\delta}_{(ns,n]}) \right) \\ & \quad + 2 \left(\ell_{(ns,nt^*]}(\hat{\delta}_{(0,nt^*]}) - \ell_{(ns,nt^*]}(\hat{\delta}_{(ns,nt^*]}) \right) + 2 \left(\ell_{(nt^*,n]}(\hat{\delta}_{(nt^*,n]}) - \ell_{(nt^*,n]}(\hat{\delta}_{(ns,n]}) \right); \end{aligned}$$

and since $\hat{\delta}_{(ns,nt^*]}$ is a maximizer of $\ell_{(ns,nt^*]}(\cdot)$, then we have the following lower bound:

$$\begin{aligned} & \geq 2 \left(\ell_{(0,ns]}(\hat{\delta}_{(0,nt^*]}) - \ell_{(0,ns]}(\hat{\delta}_{(0,ns]}) \right) + 2 \left(\ell_{(ns,nt^*]}(\hat{\delta}_{(0,nt^*]}) - \ell_{(ns,nt^*]}(\hat{\delta}_{(ns,nt^*]}) \right) \\ & \quad + 2 \left(\ell_{(nt^*,n]}(\hat{\delta}_{(nt^*,n]}) - \ell_{(nt^*,n]}(\hat{\delta}_{(ns,n]}) \right) \\ & := A_1(n, s) + A_2(n, s) + A_3(n, s), \end{aligned}$$

Invoking results in Theorem 1, we see that terms $A_1(n, s)$ and $A_2(n, s)$ converge weakly to some processes that are finite with probability 1.

We next claim that $\sup_{s \in [\gamma, t^* - \tau]} A_3(n, s) \xrightarrow{P} \infty$, i.e.

$$\lim_{n \rightarrow \infty} \mathbb{P} \left(\sup_{s \in [\gamma, t^* - \tau]} A_3(n, s) > L \right) = 1,$$

for all $L > 0$. The mean value theorem expansion allows us to write $A_3(n, s)$ as

$$2 \left(\ell_{(nt^*,n]}(\hat{\delta}_{(nt^*,n]}) - \ell_{(nt^*,n]}(\hat{\delta}_{(ns,n]}) \right) = 2u_{(nt^*,n]}(\delta_n^*(s)) \left(\hat{\delta}_{(nt^*,n]} - \hat{\delta}_{(ns,n]} \right), \quad (16)$$

for some $\delta_n^*(s)$ between $\hat{\delta}_{(ns,n]}$ and $\hat{\delta}_{(nt^*,n]}$. Since $\hat{\delta}_{(nt^*,n]}(\cdot)$ is maximized by $\hat{\delta}_{(nt^*,n]}$, we can write

$$2 \left(\ell_{(nt^*,n]}(\hat{\delta}_{(nt^*,n]}) - \inf_{s \in [\gamma, t^* - \tau]} \ell_{(nt^*,n]}(\hat{\delta}_{(ns,n]}) \right) = \sup_{s \in [\gamma, t^* - \tau]} 2 |u_{(nt^*,n]}(\delta_n^*(s))| \cdot \left| \hat{\delta}_{(nt^*,n]} - \hat{\delta}_{(ns,n]} \right|$$

Our proof consists of two parts, and we will show that as $n \rightarrow \infty$,

- (1) $\mathbb{P} \left(\inf_{s \in [\gamma, t^* - \tau]} \left| \hat{\delta}_{(nt^*,n]} - \hat{\delta}_{(ns,n]} \right| > \epsilon \right) \rightarrow 1;$
- (2) $\sup_{s \in [\gamma, t^* - \tau]} |u_{(nt^*,n]}(\delta_n^*(s))| \xrightarrow{P} \infty.$

We now focus on (1) and consider the term $\left| \hat{\delta}_{(nt^*,n]} - \hat{\delta}_{(ns,n]} \right|$. Note that $u_{(ns,n]}(\delta) = u_{(ns,nt^*]}(\delta) + u_{(nt^*,n]}(\delta)$, and Lemma 3 gives that

$$\sup_{\lambda \in [\eta, K]} |n^{-1}u_{(ns,nt^*]}(\lambda) - (t^* - s)U_1(\lambda)| \xrightarrow{P} 0 \quad \text{and} \quad \sup_{\lambda \in [\eta, K]} |n^{-1}u_{(nt^*,n]}(\lambda) - (1 - t^*)U_2(\lambda)| \xrightarrow{P} 0, \quad (17)$$

where $U_1(\lambda)$ and $U_2(\lambda)$ are the same as $U(\lambda)$ in Lemma 3, except $p_{>i}(\delta)$ is evaluated at δ_1 and δ_2 , respectively. Hence,

$$\sup_{\lambda \in [\eta, K]} |n^{-1}u_{(ns, n]}(\lambda) - V(\lambda)| \xrightarrow{P} 0, \quad (18)$$

where we set $V(\lambda) := (t^* - s)U_1(\lambda) + (1 - t^*)U_2(\lambda)$. Also note that $U_1(\lambda)$ and $U_2(\lambda)$ have unique zeros at δ_1 and δ_2 , respectively, and are positive before and negative after their zeros (see Lemma 4 in Gao & van der Vaart (2017)).

In particular, $|V(\delta_2)| = |(t^* - s)U_1(\delta_2) + (1 - t^*)U_2(\delta_2)| = |(t^* - s)U_1(\delta_2)| > 0$ since $U_1(\lambda)$ has a unique zero at δ_1 and is positive beforehand. Fix $0 < \xi < |V(\delta_2)|$, and the continuity of $V(\lambda)$ thus gives the existence of a $\epsilon > 0$ such that

$$\inf_{\lambda: |\lambda - \delta_2| < 2\epsilon} |V(\lambda)| > \xi.$$

Further, since $n^{-1}u_{(ns, n]}(\hat{\delta}_{(ns, n]}) = 0$,

$$|V(\hat{\delta}_{(ns, n]})| = |V(\hat{\delta}_{(ns, n]}) - n^{-1}u_{(ns, n]}(\hat{\delta}_{(ns, n]})| \leq \sup_{\lambda \in [\epsilon, K]} \left| \frac{1}{n}u_{(ns, n]}(\lambda) - V(\lambda) \right|. \quad (19)$$

Therefore, we conclude from (18) that with probability tending towards 1,

$$|V(\hat{\delta}_{(ns, n]})| \leq \sup_{\lambda \in [\epsilon, K]} \left| \frac{1}{n}u_{(ns, n]}(\lambda) - V(\lambda) \right| \leq \xi < \inf_{\lambda: |\lambda - \delta_2| < 2\epsilon} |V(\lambda)|,$$

which further implies $\mathbb{P}(|\hat{\delta}_{(ns, n]} - \delta_2| > 2\epsilon) \rightarrow 1$. Meanwhile, by the consistency of $\hat{\delta}_{(nt^*, n]}$, we have

$$\mathbb{P}(|\hat{\delta}_{(nt^*, n]} - \delta_2| < \epsilon) \rightarrow 1.$$

Hence, we see that as $n \rightarrow \infty$,

$$\mathbb{P}\left(\inf_{s \in [\gamma, t^* - \tau]} |\hat{\delta}_{(nt^*, n]} - \hat{\delta}_{(ns, n]}| > \epsilon\right) \rightarrow 1. \quad (20)$$

We next show that $\sup_{s \in [\gamma, t^* - \tau]} |u_{(nt^*, n]}(\delta_n^*(s))| \xrightarrow{P} \infty$. Let $\mathcal{B}_r(x)$ denote the open ball of radius r centered at x . Note that as $n \rightarrow \infty$, $\delta_n^*(s) \notin \mathcal{B}_\kappa(\delta_2)$ with high probability for some $\kappa > 0$ since $\hat{\delta}_{(nt^*, n]}$ and $\hat{\delta}_{(ns, n]}$ are well-separated with probability tending towards 1 and $\ell_{(nt^*, n]}(\cdot)$ is non-linear and maximized at $\hat{\delta}_{(nt^*, n]}$. Further,

$$\begin{aligned} |n^{-1}u_{(nt^*, n]}(\delta_n^*(s))| &\geq (1 - t^*)|U_2(\delta_n^*(s))| - \sup_{\lambda \in [\eta, K]} |n^{-1}u_{(nt^*, n]}(\lambda) - (1 - t^*)U_2(\lambda)| \\ &\geq (1 - t^*) \inf_{\lambda \notin \mathcal{B}_\kappa(\delta_2)} |U_2(\lambda)| - \sup_{\lambda \in [\eta, K]} |n^{-1}u'_{(nt^*, n]}(\lambda) + (1 - t^*)I_2(\lambda)|. \end{aligned}$$

The first term is nonzero since $U_2(\cdot)$ has a unique zero at δ_2 . The second term can be made arbitrarily small by (17). Hence

$$\sup_{s \in [\gamma, t^* - \tau]} |u_{(nt^*, n]}(\delta_n^*(s))| \xrightarrow{P} \infty. \quad (21)$$

Combining (21) with (20) gives that $-2 \log \Lambda_{nt^*} + \inf_{s \in [\gamma, t^* - \tau]} 2 \log \Lambda_{ns} \xrightarrow{P} \infty$, which implies the existence of a $\kappa > 0$ such that

$$\mathbb{P}\left(-2 \log \Lambda_{nt^*} > \sup_{s \in [\gamma, t^* - \tau]} -2 \log \Lambda_{ns} + \kappa\right) \rightarrow 1.$$

Therefore, as $n \rightarrow \infty$, the maximum becomes well-separated, and occurs at t^* so that we have

$$\hat{t}_n = n^{-1} \arg \max_{m=\lfloor n\gamma \rfloor, \dots, \lfloor n(1-\gamma) \rfloor} \Lambda_m \xrightarrow{p} t^*.$$

A.5. Proof of Theorem 3

We first observe that via a Taylor expansion of $u_{(0,nt]}(\lambda)$ around $\hat{\delta}_{(0,nt]}$

$$\begin{aligned} n^{-1/2} u_{(0,nt]}(\hat{\delta}_n) &= n^{-1/2} u_{(0,nt]}(\hat{\delta}_{(0,nt]}) + n^{-1/2} u'_{(0,nt]}(\delta_n^*)(\hat{\delta}_n - \hat{\delta}_{(0,nt]}) \\ &= n^{-1/2} u'_{(0,nt]}(\delta_n^*)(\hat{\delta}_n - \hat{\delta}_{(0,nt]}). \end{aligned}$$

where δ_n^* lies between $\hat{\delta}_n$ and $\hat{\delta}_{(0,nt]}$. Similarly to the argument made in Lemma 1,

$$-n^{-1} u'_{(0,nt]}(\delta_n^*) \xrightarrow{p} tI(\delta) \quad \text{in } D[0, 1],$$

and by (2),

$$tI(\delta) \cdot \sqrt{n} \left(\hat{\delta}_n - \hat{\delta}_{(0,nt]} \right) \Rightarrow tW(I(\delta)) - W(tI(\delta)) \quad \text{in } D[\gamma, 1],$$

which implies

$$n^{-1} u_{(0,nt]}^2(\hat{\delta}_n) \Rightarrow (tW(I(\delta)) - W(tI(\delta)))^2 \quad \text{in } D[\gamma, 1].$$

Further, Lemma 3 gives that in $D[0, 1]$,

$$-n^{-1} u'_{(0,nt]}(\hat{\delta}_n) \xrightarrow{p} tI(\delta) \quad \text{in } D[0, 1] \quad \text{and} \quad -n^{-1} u'_{(nt,n]}(\hat{\delta}_n) \xrightarrow{p} (1-t)I(\delta).$$

Define the Brownian bridge $B(t) := I^{-1/2}(\delta) (W(tI(\delta)) - tW(I(\delta)))$. Combining the previous three convergences thus gives

$$S_{nt} = -u_{(0,nt]}^2(\hat{\delta}_n) \left(\frac{1}{u'_{(0,nt]}(\hat{\delta}_n)} + \frac{1}{u'_{(nt,n]}(\hat{\delta}_n)} \right) \Rightarrow B^2(t) \left(\frac{1}{t} + \frac{1}{1-t} \right) = \frac{B^2(t)}{t(1-t)}$$

in $D[\gamma, 1-\gamma]$. Then applying the continuous mapping theorem gives

$$\sup_{t \in [\gamma, 1-\gamma]} S_{nt} \Rightarrow \sup_{t \in [\gamma, 1-\gamma]} \frac{B^2(t)}{t(1-t)} \quad \text{in } \mathbb{R}.$$